

## **C. Yield strength, tensile strength, hardness and ductility**

---



# Chapter 8

## The yield strength, tensile strength, hardness and ductility

---

### Introduction

All solids have an *elastic limit* beyond which something happens. A totally brittle solid will fracture, either suddenly (like glass) or progressively (like cement or concrete). Most engineering materials do something different; they deform *plastically* or change their shapes in a *permanent* way. It is important to know when, and how, they do this – both so that we can design structures which will withstand normal service loads without any permanent deformation, and so that we can design rolling mills, sheet presses, and forging machinery which will be strong enough to impose the desired deformation onto materials we wish to form. To study this, we pull carefully prepared samples in a tensile-testing machine, or compress them in a compression machine (which we will describe in a moment), and record the *stress* required to produce a given *strain*.

### Linear and non-linear elasticity; anelastic behaviour

Figure 8.1 shows the *stress–strain* curve of a material exhibiting *perfectly linear elastic* behaviour. This is the behaviour characterised by Hooke's Law (Chapter 3). All solids are linear elastic at small strains – by which we usually mean less than 0.001, or 0.1%. The slope of the stress–strain line, which is the same in compression as in tension, is of

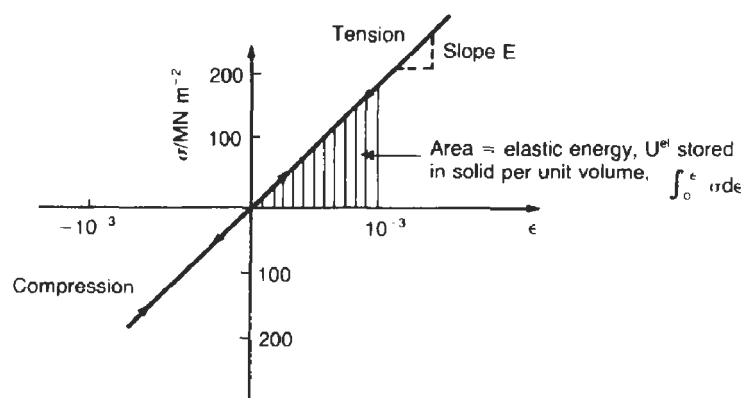


Fig. 8.1. Stress–strain behaviour for a *linear elastic solid*. The axes are calibrated for a material such as steel.

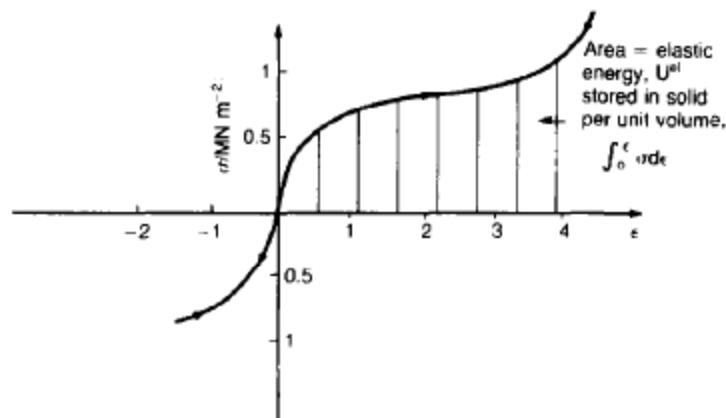


Fig. 8.2. Stress-strain behaviour for a *non-linear elastic solid*. The axes are calibrated for a material such as rubber.

course Young's Modulus,  $E$ . The area (shaded) is the elastic energy stored, per unit volume: since it is an elastic solid, we can get it all back if we unload the solid, which behaves like a linear spring.

Figure 8.2 shows a *non-linear elastic solid*. *Rubbers* have a stress-strain curve like this, extending to very large strains (of order 5). The material is still elastic: if unloaded, it follows the same path down as it did up, and all the energy stored, per unit volume, during loading is recovered on unloading – that is why catapults can be as lethal as they are.

Finally, Fig. 8.3 shows a third form of *elastic* behaviour found in certain materials. This is called *anelastic* behaviour. All solids are anelastic to a small extent: even in the régime where they are nominally elastic, the loading curve does not *exactly* follow the unloading curve, and energy is dissipated (equal to the shaded area) when the solid is cycled. Sometimes this is useful – if you wish to damp out vibrations or noise, for example; you

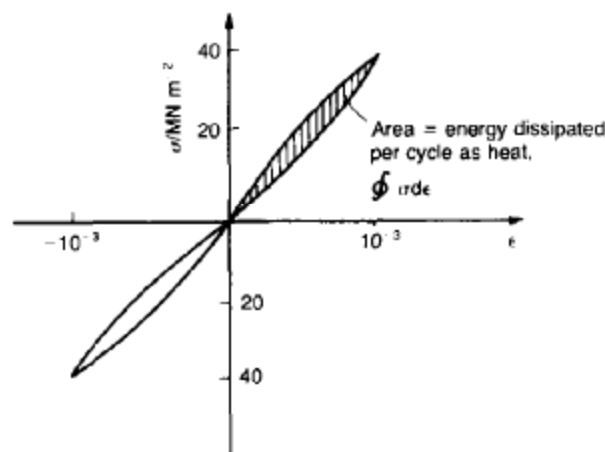


Fig. 8.3. Stress-strain behaviour for an *anelastic solid*. The axes are calibrated for fibreglass.

can do so with polymers or with soft metals (like lead) which have a high *damping capacity* (high anelastic loss). But often such damping is undesirable – springs and bells, for instance, are made of materials with the lowest possible damping capacity (spring steel, bronze, glass).

### Load-extension curves for non-elastic (plastic) behaviour

Rubbers are exceptional in behaving reversibly, or *almost* reversibly, to high strains; as we said, *almost all materials, when strained by more than about 0.001 (0.1%), do something irreversible*: and most engineering materials deform *plastically* to change their shape *permanently*. If we load a piece of ductile metal (like copper), for example in tension, we get the following relationship between the load and the extension (Fig. 8.4). This can be

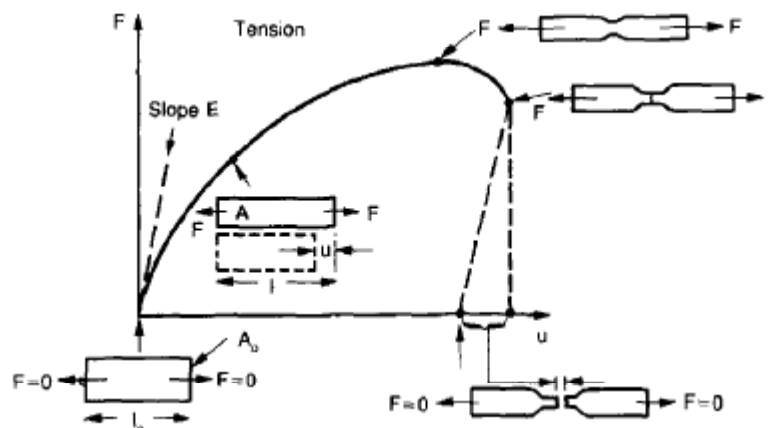


Fig. 8.4. Load–extension curve for a bar of ductile metal (e.g. annealed copper) pulled in tension.

demonstrated nicely by pulling a piece of plasticine (a ductile non-metallic material). Initially, the plasticine deforms elastically, but at a small strain begins to deform plastically, so that if the load is removed, the piece of plasticine is permanently longer than it was at the beginning of the test: it has undergone *plastic* deformation (Fig. 8.5). If you continue to pull, it continues to get longer, at the same time getting thinner because in plastic deformation *volume is conserved* (matter is just flowing from place to place). Eventually, the plasticine becomes unstable and begins to *neck* at the maximum load point in the force–extension curve (Fig. 8.4). Necking is an *instability* which we shall look at in more detail in Chapter 11. The neck then grows quite rapidly, and the load that the specimen can bear through the neck decreases until breakage takes place. The two pieces produced *after* breakage have a total length that is slightly *less* than the length *just* before breakage by the amount of the *elastic* extension produced by the terminal load.

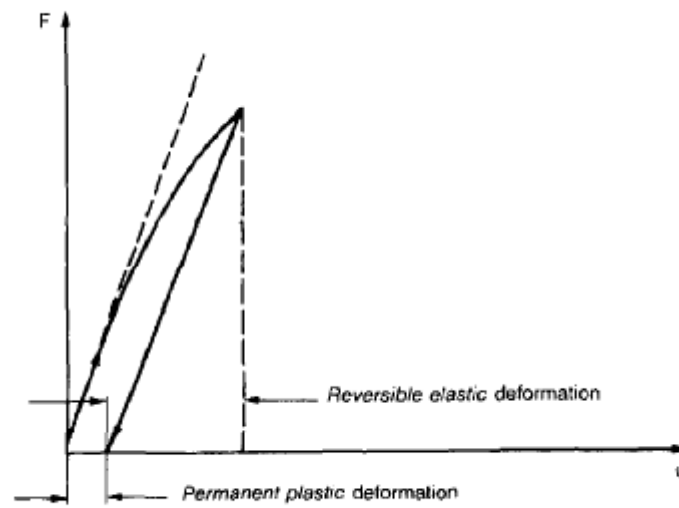


Fig. 8.5.

If we load a material in *compression*, the force–displacement curve is simply the reverse of that for tension at *small strains*, but it becomes different at larger strains. As the specimen squashes down, becoming shorter and fatter to conserve volume, the load needed to keep it flowing rises (Fig. 8.6). No instability such as necking appears, and the specimen can be squashed almost indefinitely, this process only being limited eventually by severe cracking in the specimen or the plastic flow of the compression plates.

Why this great difference in behaviour? After all, we are dealing with the same material in either case.

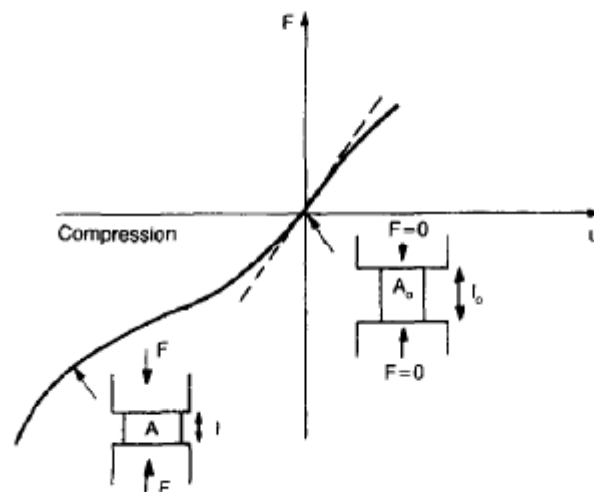


Fig. 8.6.

### True stress–strain curves for plastic flow

The apparent difference between the curves for tension and compression is due solely to the geometry of testing. If, instead of plotting load, we plot load divided by the actual area of the specimen,  $A$ , at any particular elongation or compression, the two curves become much more like one another. In other words, we simply plot true stress (see Chapter 3) as our vertical co-ordinate (Fig. 8.7). This method of plotting allows for the *thinning* of the material when pulled in tension, or the *fattening* of the material when compressed.

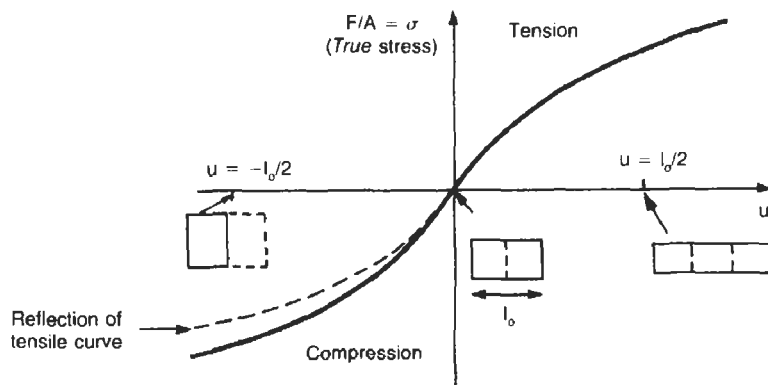


Fig. 8.7.

But the two curves still do not exactly match, as Fig. 8.7 shows. The reason is a displacement of (for example)  $u = l_0/2$  in tension and compression gives different strains; it represents a drawing out of the tensile specimen from  $l_0$  to  $1.5l_0$ , but a squashing down of the compressive specimen from  $l_0$  to  $0.5l_0$ . The material of the compressive specimen has thus undergone *much* more plastic deformation than the material in the tensile specimen, and can hardly be expected to be in the same state, or to show the same resistance to plastic deformation. The two conditions can be compared properly by taking small *strain increments*

$$\delta\epsilon = \frac{\delta u}{l} = \frac{\delta l}{l} \tag{8.1}$$

about which the state of the material is the same for either tension or compression (Fig. 8.8). This is the same as saying that a decrease in length from 100 mm ( $l_0$ ) to 99 mm ( $l$ ), or an increase in length from 100 mm ( $l_0$ ) to 101 mm ( $l$ ) both represent a 1% change in the state of the material. Actually, they do not *quite* give exactly 1% in both cases, of course, but they *do* in the limit

$$d\epsilon = \frac{dl}{l}. \tag{8.2}$$

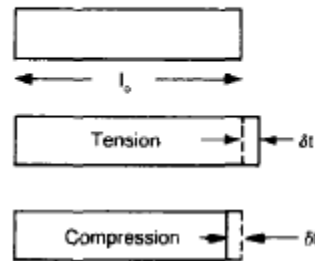


Fig. 8.8.

Then, if the stresses in compression and tension are plotted against

$$\epsilon = \int_{l_0}^l \frac{dl}{l} = \ln \left( \frac{l}{l_0} \right) \quad (8.3)$$

the two curves *exactly* mirror one another (Fig. 8.9). The quantity  $\epsilon$  is called the *true strain* (to be contrasted with the *nominal strain*  $u/l_0$  (defined in Chapter 3)) and the matching curves are *true stress/true strain* ( $\sigma/\epsilon$ ) curves. Now, a final catch. We can, from our original load-extension or load-compression curves easily calculate  $\epsilon$ , simply by knowing  $l_0$  and taking natural logs. But how do we calculate  $\sigma$ ? Because volume is conserved during plastic deformation we can write, at any strain,

$$A_0 l_0 = A l$$

provided the extent of plastic deformation is much greater than the extent of elastic deformation (this is usually the case, but the qualification must be mentioned because

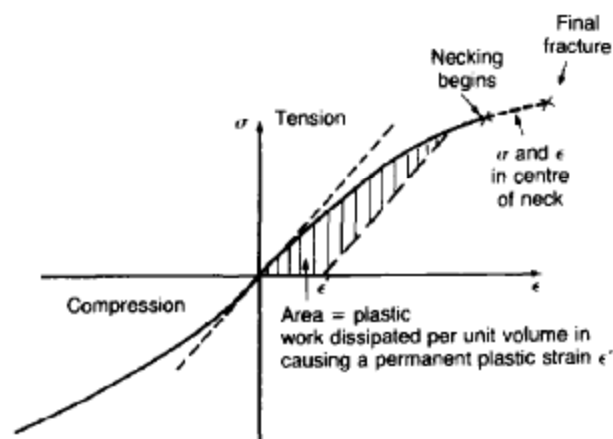


Fig. 8.9.

volume is only conserved during *elastic* deformation if Poisson's ratio  $\nu = 0.5$ ; and, as we showed in Chapter 3, it is near 0.33 for most materials). Thus

$$A = \frac{A_0 l_0}{l} \quad (8.4)$$

and

$$\sigma = \frac{F}{A} = \frac{Fl}{A_0 l_0}, \quad (8.5)$$

all of which we know or can measure easily.

### Plastic work

When metals are rolled or forged, or drawn to wire, or when polymers are injection-moulded or pressed or drawn, energy is absorbed. The work done on a material to change its shape permanently is called the *plastic work*; its value, per unit volume, is the area of the cross-hatched region shown in Fig. 8.9; it may easily be found (if the stress-strain curve is known) for any amount of permanent plastic deformation,  $\epsilon'$ . Plastic work is important in metal- and polymer-forming operations because it determines the forces that the rolls, or press, or moulding machine must exert on the material.

### Tensile testing

The plastic behaviour of a material is usually measured by conducting a tensile test. Tensile testing equipment is standard in all engineering laboratories. Such equipment produces a load/displacement ( $F/u$ ) curve for the material, which is then converted to a nominal stress/nominal strain, or  $\sigma_n/\epsilon_n$ , curve (Fig. 8.10), where

$$\sigma_n = \frac{F}{A_0} \quad (8.6)$$

and

$$\epsilon_n = \frac{u}{l_0} \quad (8.7)$$

(see Chapter 3, and above). Naturally, because  $A_0$  and  $l_0$  are constant, the *shape* of the  $\sigma_n/\epsilon_n$  curve is identical to that of the load-extension curve. But the  $\sigma_n/\epsilon_n$  plotting method allows one to compare data for specimens having different (though now standardised)  $A_0$  and  $l_0$ , and thus to examine the properties of *material*, unaffected by specimen size. The advantage of keeping the stress in *nominal* units and not converting to *true* stress (as shown above) is that the onset of necking can clearly be seen on the  $\sigma_n/\epsilon_n$  curve.

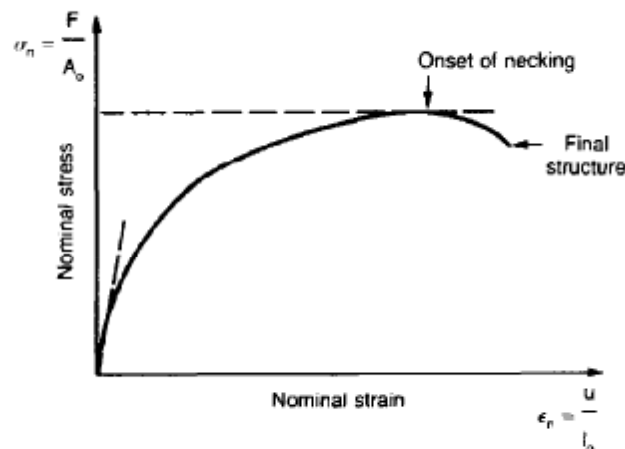


Fig. 8.10

Now, let us define the quantities usually listed as the results of a *tensile test*. The easiest way to do this is to show them on the  $\sigma_n/\epsilon_n$  curve itself (Fig. 8.11). They are:

- $\sigma_y$  Yield strength ( $F/A_0$  at onset of plastic flow).
- $\sigma_{0.1\%}$  0.1% Proof stress ( $F/A_0$  at a permanent strain of 0.1%) (0.2% proof stress is often quoted instead. Proof stress is useful for characterising yield of a material that yields gradually, and does not show a distinct yield point.)
- $\sigma_{TS}$  Tensile strength ( $F/A_0$  at onset of necking).
- $\epsilon_f$  (Plastic) strain after fracture, or tensile ductility. The broken pieces are put together and measured, and  $\epsilon_f$  calculated from  $(l - l_0)/l_0$ , where  $l$  is the length of the assembled pieces.

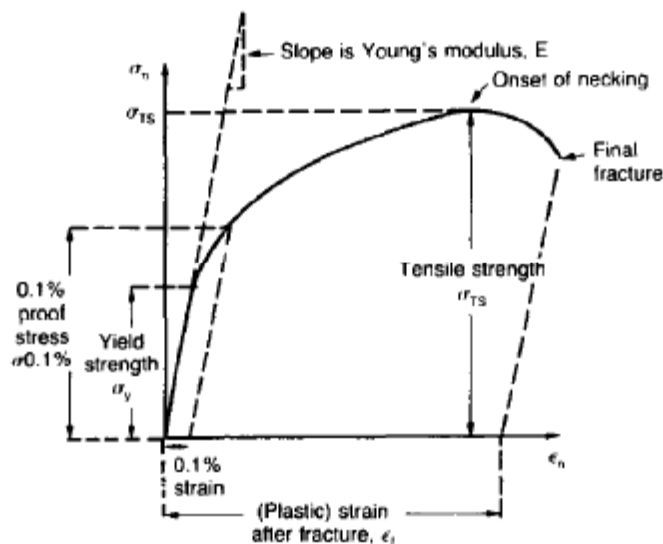


Fig. 8.11.

## Data

Data for the *yield strength*, *tensile strength* and the *tensile ductility* are given in Table 8.1 and shown on the bar-chart (Fig. 8.12). Like moduli, they span a range of about  $10^6$ : from about  $0.1 \text{ MN m}^{-2}$  (for polystyrene foams) to nearly  $10^5 \text{ MN m}^{-2}$  (for diamond).

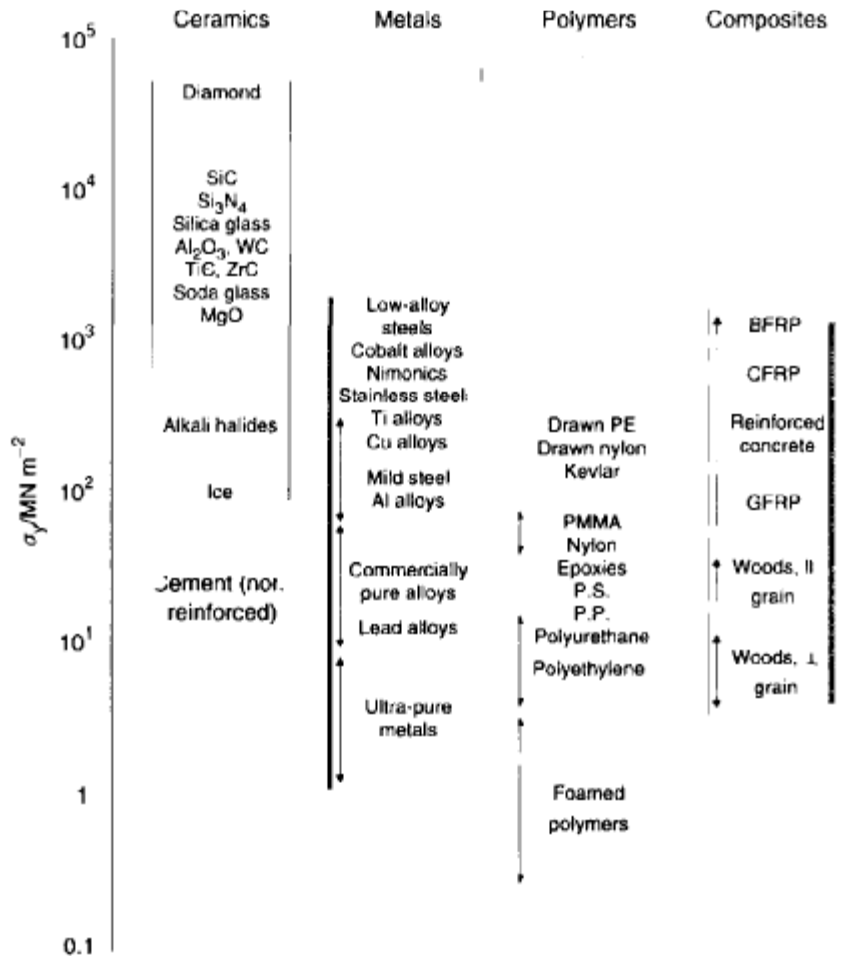


Fig. 8.12. Bar-chart of data for yield strength,  $\sigma_y$ .

Most ceramics have enormous yield stresses. In a tensile test, at room temperature, ceramics almost all fracture long before they yield: this is because their fracture toughness, which we will discuss later, is very low. Because of this, you cannot measure the yield strength of a ceramic by using a tensile test. Instead, you have to use a test which somehow suppresses fracture: a compression test, for instance. The best and easiest is the hardness test: the data shown here are obtained from hardness tests, which we shall discuss in a moment.

Pure metals are very soft indeed, and have a high ductility. This is what, for centuries, has made them so attractive at first for jewellery and weapons, and then for other implements and structures: they can be *worked* to the shape that you want them in; furthermore, their ability to work-harden means that, after you have finished, the

**Table 8.1** Yield strength,  $\sigma_y$ , tensile strength,  $\sigma_{TS}$ , and tensile ductility,  $\epsilon_f$ 

Material	$\sigma_y/\text{MN m}^{-2}$	$\sigma_{TS}/\text{MN m}^{-2}$	$\epsilon_f$
Diamond	50 000	–	0
Silicon carbide, SiC	10 000	–	0
Silicon nitride, Si <sub>3</sub> N <sub>4</sub>	8 000	–	0
Silica glass, SiO <sub>2</sub>	7 200	–	0
Tungsten carbide, WC	6 000	–	0
Niobium carbide, NbC	6 000	–	0
Alumina, Al <sub>2</sub> O <sub>3</sub>	5 000	–	0
Beryllia, BeO	4 000	–	0
Mullite	4 000	–	0
Titanium carbide, TiC	4 000	–	0
Zirconium carbide, ZrC	4 000	–	0
Tantalum carbide, TaC	4 000	–	0
Zirconia, ZrO <sub>2</sub>	4 000	–	0
Soda glass (standard)	3 600	–	0
Magnesia, MgO	3 000	–	0
Cobalt and alloys	180–2000	500–2500	0.01–6
Low-alloy steels (water-quenched and tempered)	500–1980	680–2400	0.02–0.3
Pressure-vessel steels	1500–1900	1500–2000	0.3–0.6
Stainless steels, austenitic	286–500	760–1280	0.45–0.65
Boron/epoxy composites (tension–compression)	–	725–1730	–
Nickel alloys	200–1600	400–2000	0.01–0.6
Nickel	70	400	0.65
Tungsten	1 000	1510	0.01–0.6
Molybdenum and alloys	560–1450	665–1650	0.01–0.36
Titanium and alloys	180–1320	300–1400	0.06–0.3
Carbon steels (water-quenched and tempered)	260–1300	500–1880	0.2–0.3
Tantalum and alloys	330–1090	400–1100	0.01–0.4
Cast irons	220–1030	400–1200	0–0.18
Copper alloys	60–960	250–1000	0.01–0.55
Copper	60	400	0.55
Cobalt/tungsten carbide cermets	400–900	900	0.02
CFRPs (tension–compression)	–	670–640	–
Brasses and bronzes	70–640	230–890	0.01–0.7
Aluminium alloys	100–627	300–700	0.05–0.3
Aluminium	40	200	0.5
Stainless steels, ferritic	240–400	500–800	0.15–0.25
Zinc alloys	160–421	200–500	0.1–1.0
Concrete, steel reinforced (tension or compression)	–	410	0.02
Alkali halides	200–350	–	0
Zirconium and alloys	100–365	240–440	0.24–0.37
Mild steel	220	430	0.18–0.25
Iron	50	200	0.3
Magnesium alloys	80–300	125–380	0.06–0.20
GFRPs	–	100–300	–
Beryllium and alloys	34–276	380–620	0.02–0.10
Gold	40	220	0.5
PMMA	60–110	110	0.03–0.05
Epoxies	30–100	30–120	–
Polyimides	52–90	–	–

Table 8.1 (Continued)

Material	$\sigma_y/\text{MNm}^{-2}$	$\sigma_{TS}/\text{MNm}^{-2}$	$\epsilon_f$
Nylons	49–87	100	–
Ice	85	–	0
Pure ductile metals	20–80	200–400	0.5–1.5
Polystyrene	34–70	40–70	–
Silver	55	300	0.6
ABS/polycarbonate	55	60	–
Common woods (compression,    to grain)	–	35–55	–
Lead and alloys	11–55	14–70	0.2–0.8
Acrylic/PVC	45–48	–	–
Tin and alloys	7–45	14–60	0.3–0.7
Polypropylene	19–36	33–36	–
Polyurethane	26–31	58	–
Polyethylene, high density	20–30	37	–
Concrete, non-reinforced, compression	20–30	–	0
Natural rubber	–	30	5.0
Polyethylene, low density	6–20	20	–
Common woods (compression, $\perp$ to grain)	–	4–10	–
Ultrapure f.c.c. metals	1–10	200–400	1–2
Foamed polymers, rigid	0.2–10	0.2–10	0.1–1
Polyurethane foam	1	1	0.1–1

metal is much stronger than when you started. By alloying, the strength of metals can be further increased, though – in yield strength – the strongest metals still fall short of most ceramics.

Polymers, in general, have lower yield strengths than metals. The very strongest (and, at present, these are produced only in small quantities, and are expensive) barely reach the strength of aluminium alloys. They can be strengthened, however, by making composites out of them: GFRP has a strength only slightly inferior to aluminium, and CFRP is substantially stronger.

### The hardness test

This consists of loading a pointed diamond or a hardened steel ball and pressing it into the surface of the material to be examined. The further into the material the ‘indenter’ (as it is called) sinks, the *softer* is the material and the lower its yield strength. The *true hardness* is defined as the load ( $F$ ) divided by the projected area of the ‘indent’,  $A$ . (The Vickers hardness,  $H_v$ , unfortunately was, and still is, defined as  $F$  divided by the total surface area of the ‘indent’. Tables are available to relate  $H$  to  $H_v$ .)

The yield strength can be found from the relation (derived in Chapter 11)

$$H = 3\sigma_y \quad (8.8)$$

but a correction factor is needed for materials which work-harden appreciably.

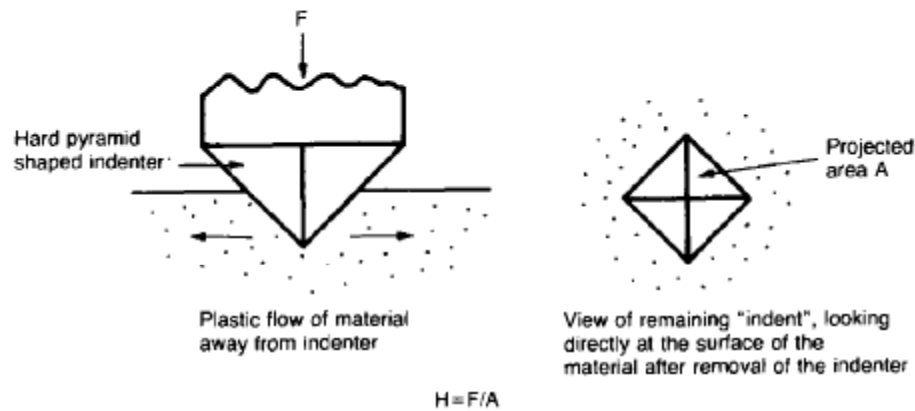


Fig. 8.13. The hardness test for yield strength.

As well as being a good way of measuring the yield strengths of materials like ceramics, as we mentioned above, the hardness test is also a very simple and cheap *non-destructive test* for  $\sigma_y$ . There is no need to go to the expense of making tensile specimens, and the hardness indenter is so small that it scarcely damages the material. So it can be used for routine batch tests on materials to see if they are up to specification on  $\sigma_y$  without damaging them.

### Further reading

K. J. Pascoe, *An Introduction to the Properties of Engineering Materials*, 3rd edition, Van Nostrand, 1978, Chap. 12.  
 Smithells' *Metals Reference Book*, 7th edition, Butterworth-Heinemann, 1992 (for data).

### Revision of the terms mentioned in this chapter, and some useful relations

$\sigma_n$ , nominal stress

$$\sigma_n = F/A_0. \quad (8.9)$$

$\sigma$ , true stress

$$\sigma = F/A. \quad (8.10)$$

$\epsilon_n$ , nominal strain

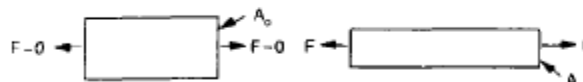


Fig. 8.14.

$$\epsilon_n = \frac{u}{l_0}, \text{ or } \frac{l - l_0}{l_0}, \text{ or } \frac{l}{l_0} - 1. \quad (8.11)$$

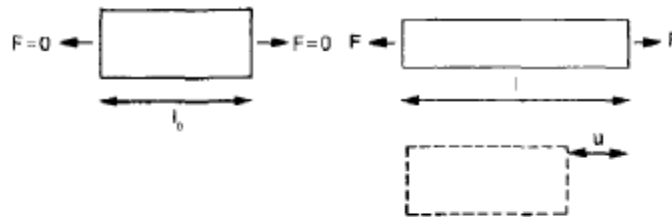


Fig. 8.15.

**Relations between  $\sigma_{nr}$ ,  $\sigma$ , and  $\epsilon_n$**

Assuming constant volume (valid if  $\nu = 0.5$  or, if not, plastic deformation  $\gg$  elastic deformation):

$$A_0 l_0 = Al; \quad A_0 = \frac{Al}{l_0} = A(1 + \epsilon_n). \quad (8.12)$$

Thus

$$\sigma = \frac{F}{A} = \frac{F}{A_0} (1 + \epsilon_n) = \sigma_n (1 + \epsilon_n). \quad (8.13)$$

**$\epsilon$ , true strain and the relation between  $\epsilon$  and  $\epsilon_n$**

$$\epsilon = \int_{l_0}^l \frac{dl}{l} = \ln \left( \frac{l}{l_0} \right). \quad (8.14)$$

Thus

$$\epsilon = \ln (1 + \epsilon_n). \quad (8.15)$$

**Small strain condition**

For small  $\epsilon_n$

$$\epsilon \approx \epsilon_n, \text{ from } \epsilon = \ln (1 + \epsilon_n), \quad (8.16)$$

$$\sigma \approx \sigma_n, \text{ from } \sigma = \sigma_n (1 + \epsilon_n). \quad (8.17)$$

Thus, when dealing with most *elastic* strains (but not in rubbers), it is immaterial whether  $\epsilon$  or  $\epsilon_n$ , or  $\sigma$  or  $\sigma_n$ , are chosen.

### Energy

The energy expended in deforming a material *per unit volume* is given by the area under the stress-strain curve. For example,

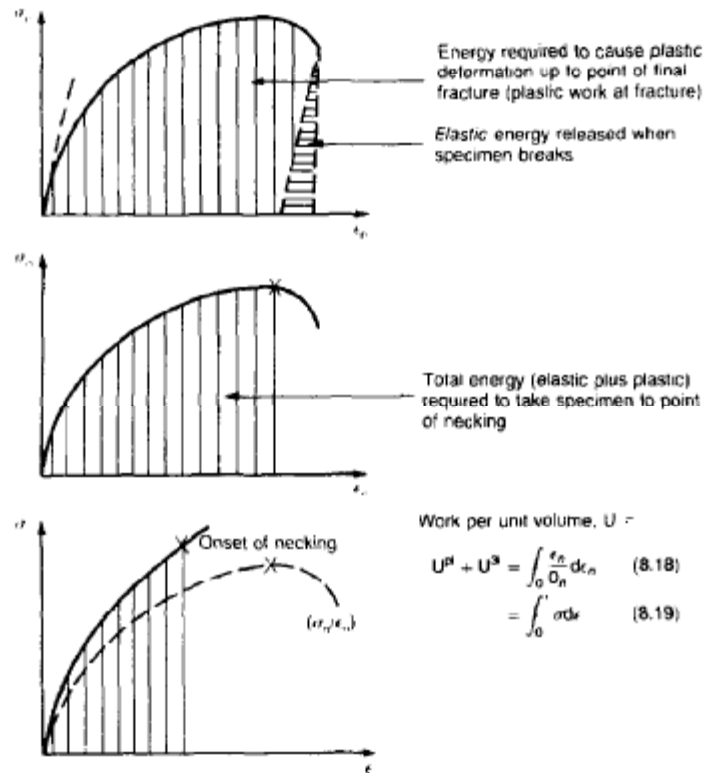


Fig. 8.16.

For *linear elastic strains*, and *only* linear elastic strains,

$$\frac{\sigma_n}{\epsilon_n} = E, \text{ and } U^{el} = \int \sigma_n d\epsilon_n = \int \sigma_n \frac{d\sigma_n}{E} = \left\{ \frac{\sigma_n^2}{2E} \right\}. \quad (8.20)$$

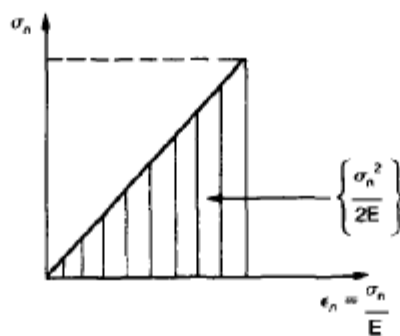


Fig. 8.17.

**Elastic limit**

In a tensile test, as the load increases, the specimen at first is strained *elastically*, that is reversibly. Above a limiting stress – the elastic limit – some of the strain is permanent; this is *plastic* deformation.

**Yielding**

The change from elastic to measurable plastic deformation.

**Yield strength**

The nominal stress at yielding. In many materials this is difficult to spot on the stress–strain curve and in such cases it is better to use a proof stress.

**Proof stress**

The stress which produces a permanent strain equal to a specified percentage of the specimen length. A common proof stress is one corresponding to 0.1% permanent strain.

**Strain hardening (work-hardening)**

The increase in stress needed to produce further strain in the plastic region. Each strain increment strengthens or hardens the material so that a larger stress is needed for further strain.

$\sigma_{TS}$ , tensile strength (in old books, ultimate tensile strength, or UTS)

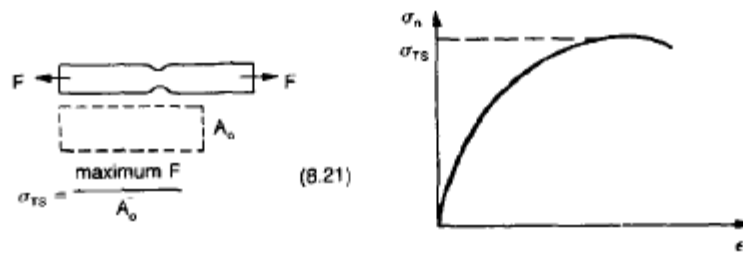


**Fig. 8.18.**

$\epsilon_f$ , strain after fracture, or tensile ductility

The permanent extension in length (measured by fitting the broken pieces together) expressed as a percentage of the original gauge length.

$$\left\{ \frac{l_{\text{break}} - l_0}{l_0} \right\} \times 100. \tag{8.22}$$

$$\left\{ \frac{A_0 - A_{\text{break}}}{A_0} \right\} \times 100 \quad (8.23)$$


The diagram shows a tensile specimen with a central necked region. The original cross-sectional area is labeled  $A_0$  and the area at the fracture point is labeled  $A_{\text{break}}$ . The specimen is shown in a state of necking, with the fracture occurring at the narrowest point.

Fig. 8.19.

### Reduction in area at break

The maximum decrease in cross-sectional area at the fracture expressed as a percentage of the original cross-sectional area.

Strain after fracture and percentage reduction in area are used as measures of ductility, i.e. the ability of a material to undergo large plastic strain under stress before it fractures.

# Chapter 9

## Dislocations and yielding in crystals

---

### Introduction

In the last chapter we examined data for the yield strengths exhibited by materials. But what would we expect? From our understanding of the structure of solids and the stiffness of the bonds between the atoms, can we estimate what the yield strength should be? A simple calculation (given in the next section) overestimates it grossly. This is because real crystals contain defects, *dislocations*, which move easily. When they move, the crystal deforms; the stress needed to move them is the yield strength. Dislocations are the *carriers* of deformation, much as electrons are the carriers of charge.

### The strength of a perfect crystal

As we showed in Chapter 6 (on the modulus), the slope of the interatomic force–distance curve at the equilibrium separation is proportional to Young’s modulus  $E$ . Interatomic forces typically drop off to negligible values at a distance of separation of the atom centres of  $2r_0$ . The maximum in the force–distance curve is typically reached at  $1.25r_0$  separation, and if the stress applied to the material is sufficient to exceed this maximum force per *bond*, fracture is bound to occur. We will denote the stress at which this bond rupture takes place by  $\bar{\sigma}$ , the *ideal strength*; a material cannot be stronger than this. From Fig. 9.1

$$\begin{aligned}\sigma &= E\epsilon, \\ 2\bar{\sigma} &\approx E \frac{0.25r_0}{r_0} \approx \frac{E}{4}, \\ \bar{\sigma} &\approx \frac{E}{8}.\end{aligned}\tag{9.1}$$

More refined estimates of  $\bar{\sigma}$  are possible, using real interatomic potentials (Chapter 4): they give about  $E/15$  instead of  $E/8$ .

Let us now see whether materials really show this strength. The bar-chart (Fig. 9.2) shows values of  $\sigma_y/E$  for materials. The heavy broken line at the top is drawn at the level  $\sigma/E = 1/15$ . Glasses, and some ceramics, lie close to this line – they exhibit their ideal strength, and we could not expect them to be stronger than this. Most polymers, too, lie near the line – although they have low yield strengths, these are low because the *moduli* are low.

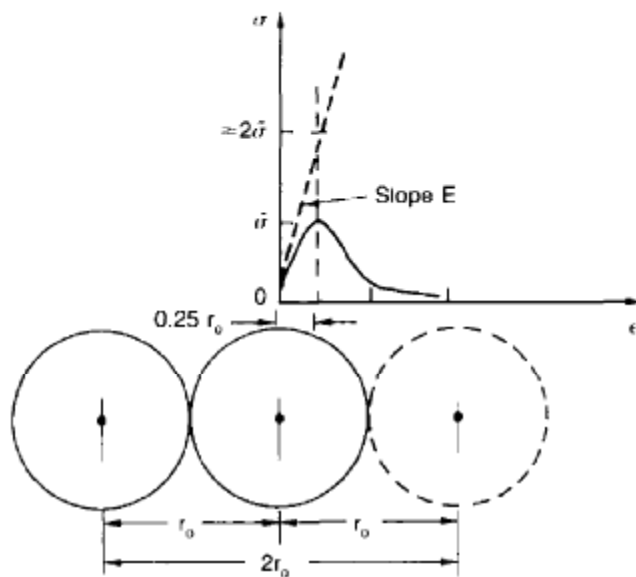


Fig. 9.1. The ideal strength,  $\bar{\sigma}$ .

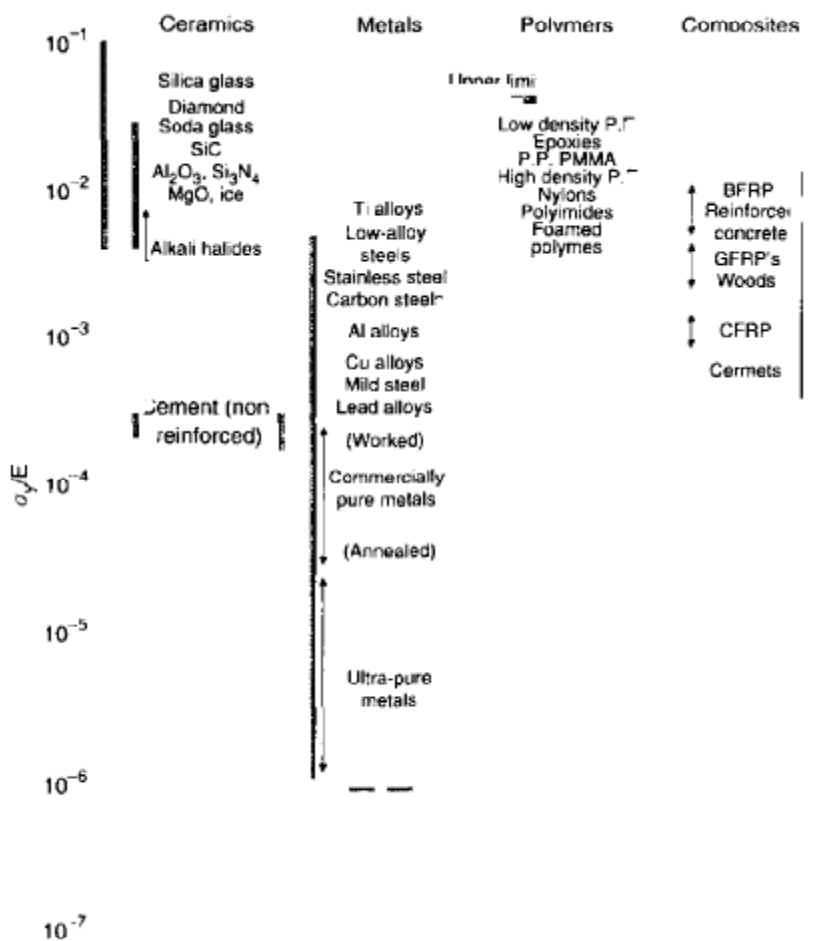


Fig. 9.2. Bar-chart of data for normalised yield strength,  $\sigma_y/E$ .

All metals, on the other hand, have yield strengths far below the levels predicted by our calculation – as much as a factor of  $10^5$  smaller. Even ceramics, many of them, yield at stresses which are as much as a factor of 10 below their ideal strength. Why is this?

## Dislocations in crystals

In Chapter 5 we said that many important engineering materials (e.g. metals) were normally made up of crystals, and explained that a perfect crystal was an assembly of *atoms packed together in a regularly repeating pattern*.

But crystals (like everything in this world) are not perfect; they have *defects* in them. Just as the strength of a chain is determined by the strength of the weakest link, so the strength of a crystal – and thus of our material – is usually limited by the defects that are present in it. The *dislocation* is a particular type of defect that has the effect of allowing materials to deform plastically (that is, they yield) at stress levels that are much less than  $\bar{\sigma}$ .

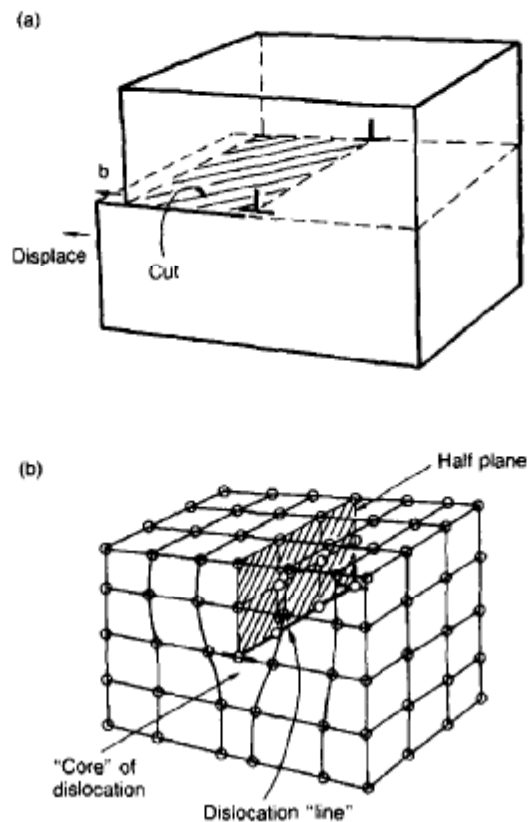
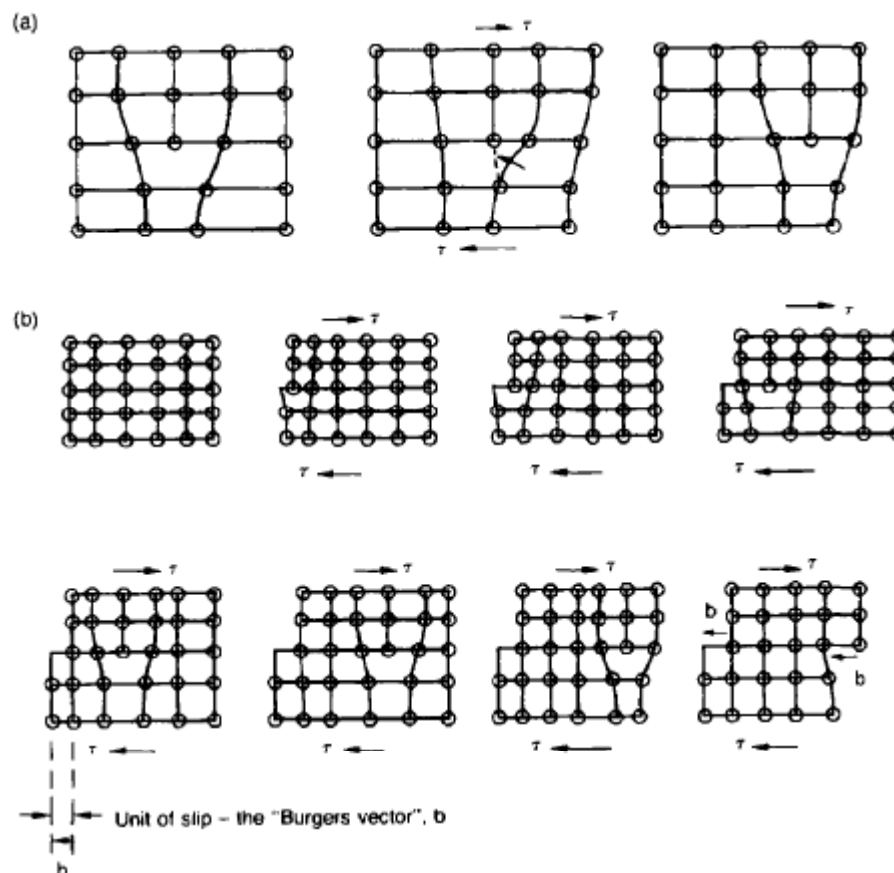


Fig. 9.3. An edge dislocation, (a) viewed from a continuum standpoint (i.e. ignoring the atoms) and (b) showing the positions of the atoms near the dislocation.

Figure 9.3(a) shows an *edge dislocation* from a continuum viewpoint (i.e. ignoring the atoms). Such a dislocation is made in a block of material by cutting the block up to the line  $\perp - \perp$ , then displacing the material below the cut relative to that above by a distance  $b$  (the atom size) normal to the line  $\perp - \perp$ , and finally gluing the cut-and-displaced surfaces back together. The result, on an atomic scale, is shown in the adjacent diagram (Fig. 9.3(b)); the material in the middle of the block now contains a *half-plane* of atoms, with its lower edge lying along the line  $\perp - \perp$ : the *dislocation line*. This defect is called an edge dislocation because it is formed by the edge of the half-plane of atoms; and it is written briefly by using the symbol  $\perp$ .

Dislocation motion produces plastic strain. Figure 9.4 shows how the atoms rearrange as the dislocation moves through the crystal, and that, when one dislocation moves entirely through a crystal, the lower part is displaced under the upper by the distance  $b$  (called the Burgers vector). The same process is drawn, without the atoms, and using the symbol  $\perp$  for the position of the dislocation line, in Fig. 9.5. The way in



**Fig. 9.4.** How an edge dislocation moves through a crystal. (a) Shows how the atomic bonds at the centre of the dislocation break and reform to allow the dislocation to move. (b) Shows a complete sequence for the introduction of a dislocation into a crystal from the left-hand side, its migration through the crystal, and its expulsion on the right-hand side; this process causes the lower half of the crystal to slip by a distance  $b$  under the upper half.

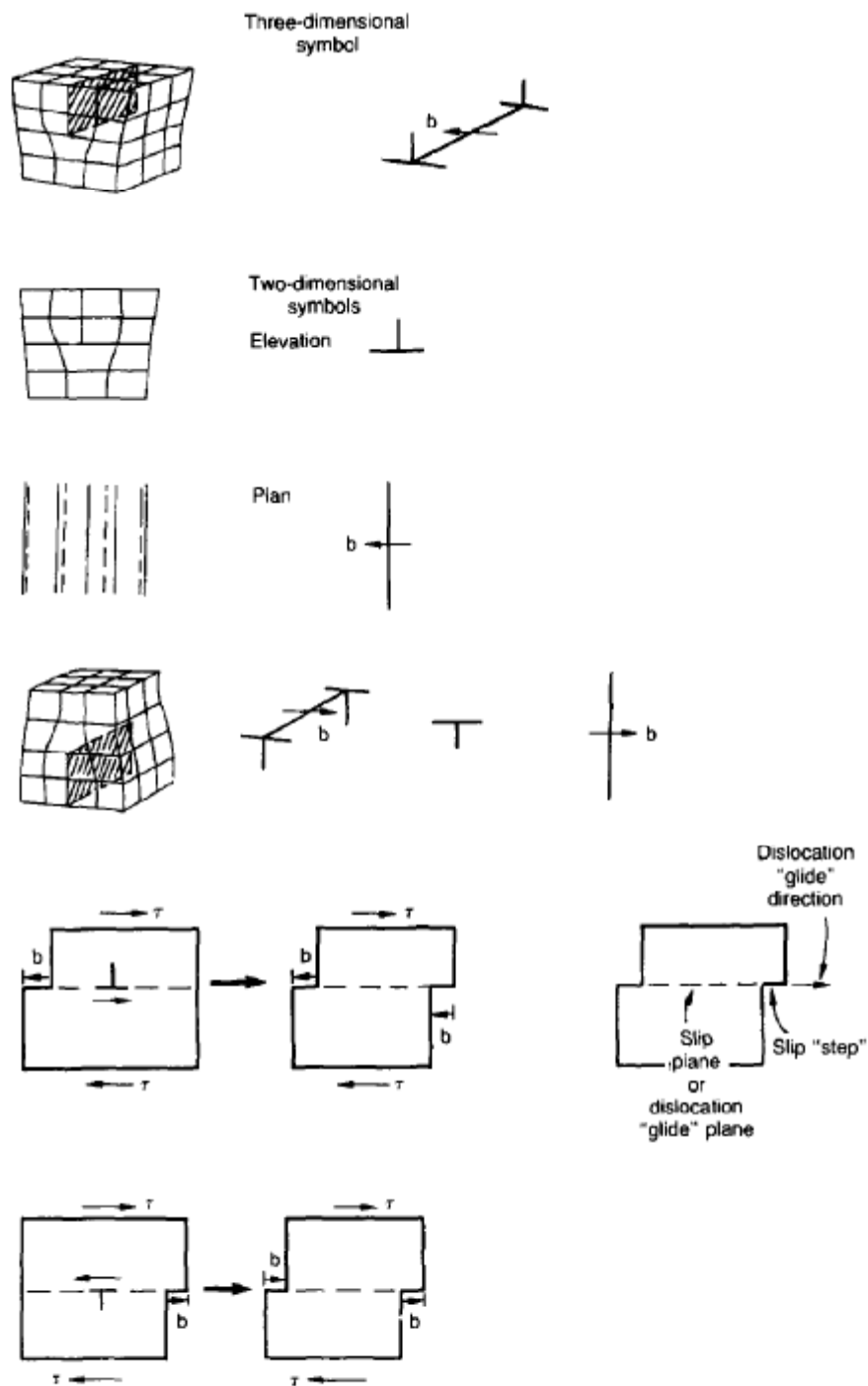


Fig. 9.5. Edge-dislocation conventions.

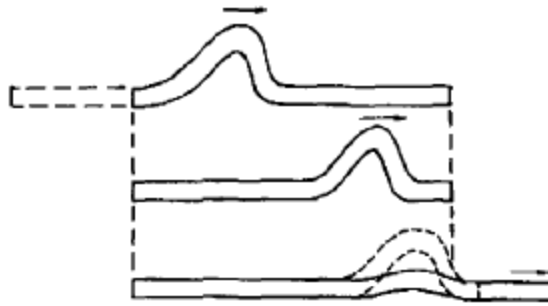


Fig. 9.6. The 'carpet-ruck' analogy of an edge dislocation.

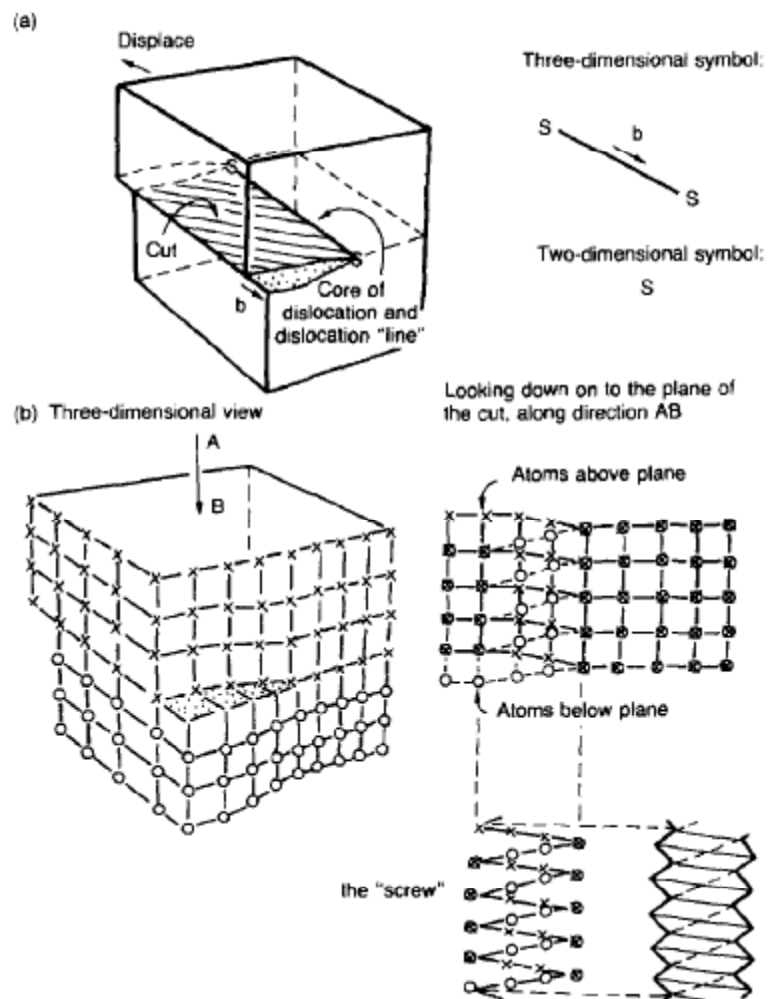


Fig. 9.7. A screw dislocation, (a) viewed from a continuum standpoint and (b) showing the atom positions.

which this dislocation works can be likened to the way in which a ballroom carpet can be moved across a large dance floor simply by moving rucks along the carpet – a very much easier process than pulling the whole carpet across the floor at one go.

In making the edge dislocation of Fig. 9.3 we could, after making the cut, have displaced the lower part of the crystal under the upper part in a direction *parallel* to the bottom of the cut, instead of normal to it. Figure 9.7 shows the result; it, too, is a dislocation, called a *screw dislocation* (because it converts the planes of atoms into a helical surface, or screw). Like an edge dislocation, it produces plastic strain when it

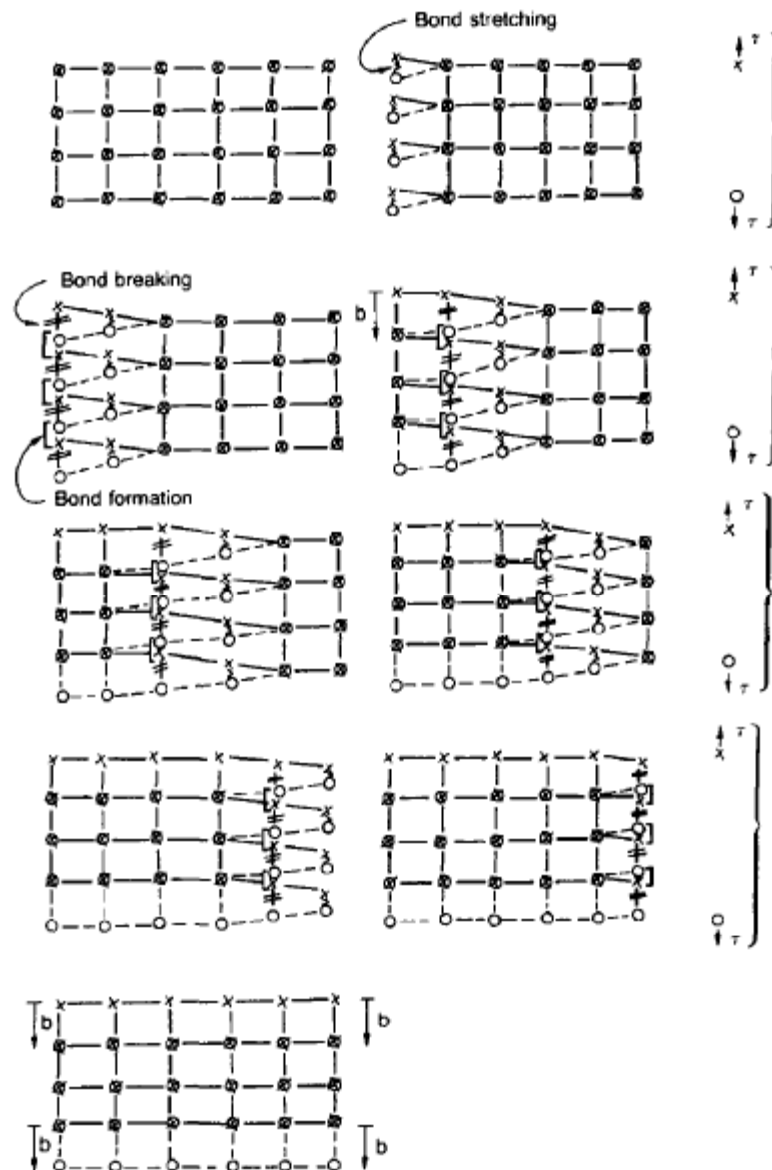


Fig. 9.8. Sequence showing how a screw dislocation moves through a crystal causing the lower half of the crystal (o) to slip by a distance  $b$  under the upper half (x).

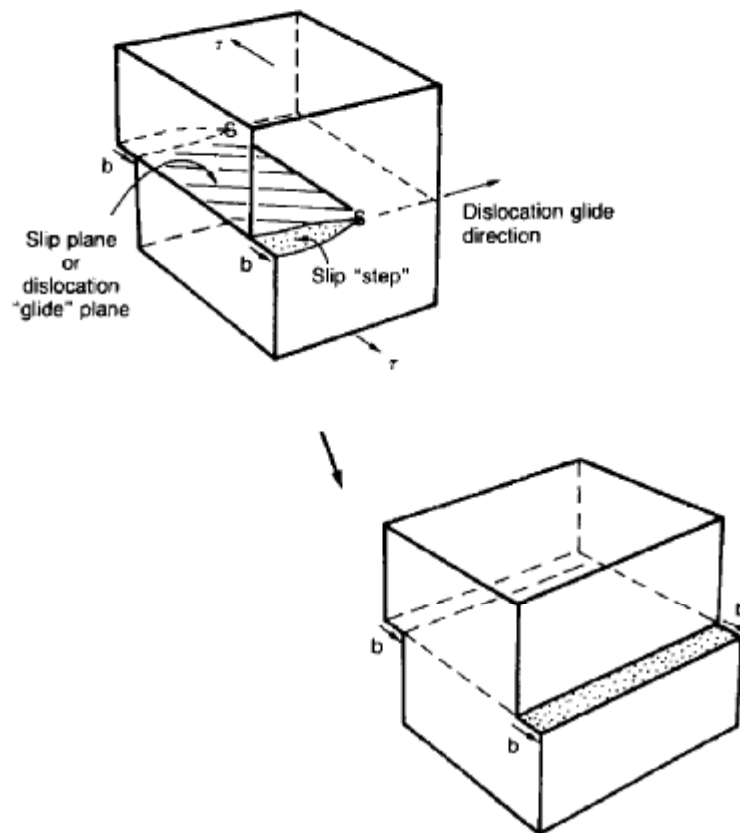


Fig. 9.9. Screw-dislocation conventions.

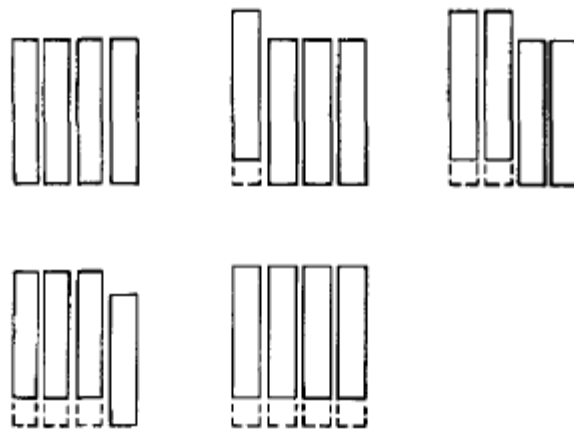


Fig. 9.10. The 'planking' analogy of the screw dislocation. Imagine four planks resting side by side on a factory floor. It is much easier to slide them across the floor one at a time than all at the same time.



**Fig. 9.11.** An electron microscope picture of dislocation lines in stainless steel. The picture was taken by firing electrons through a very thin slice of steel about 100 nm thick. The dislocation lines here are only about 1000 atom diameters long because they have been 'chopped off' where they meet the top and bottom surfaces of the thin slice. But a sugar-cube-sized piece of any engineering alloy contains about  $10^5$  km of dislocation line. (Courtesy of Dr. Peter Southwick.)

moves (Figs 9.8, 9.9, 9.10). Its geometry is a little more complicated but its properties are otherwise just like those of the edge. Any dislocation, in a real crystal, is either a screw or an edge; or can be thought of as little steps of each. Dislocations can be seen by electron microscopy. Figure 9.11 shows an example.

### The force acting on a dislocation

A shear stress ( $\tau$ ) exerts a force on a dislocation, pushing it through the crystal. For yielding to take place, this force must be great enough to overcome the *resistance* to the motion of the dislocation. This resistance is due to intrinsic friction opposing dislocation motion, plus contributions from alloying or work-hardening; they are discussed in detail in the next chapter. Here we show that the magnitude of the force is  $\tau b$  per unit length of dislocation.

We prove this by a virtual work calculation. We equate the work done by the applied stress when the dislocation moves completely through the crystal to the work done against the force  $f$  opposing its motion (Fig. 9.12). The upper part is displaced relative to the lower by the distance  $b$ , and the applied stress does work  $(\tau l_1 l_2) \times b$ . In moving

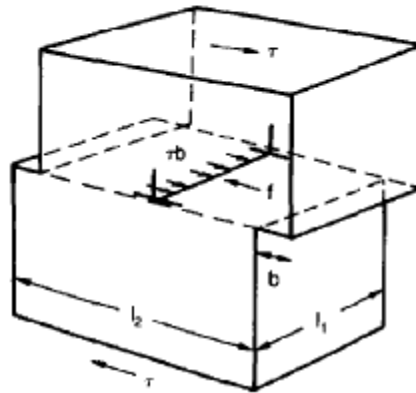


Fig. 9.12. The force acting on a dislocation.

through the crystal, the dislocation travels a distance  $l_2$ , doing work against the resistance,  $f$  per unit length, as it does so; this work is  $fl_1l_2$ . Equating the two gives

$$\tau b = f. \quad (9.2)$$

This result holds for any dislocation – edge, screw or a mixture of both.

### Other properties of dislocations

There are two remaining properties of dislocations that are important in understanding the plastic deformation of materials. These are:

- Dislocations always glide on crystallographic planes, as we might imagine from our earlier drawings of edge-dislocation motion. In f.c.c. crystals, for example, the dislocations glide on {111} planes, and therefore plastic shearing takes place on {111} in f.c.c. crystals.
- The atoms near the core of a dislocation are displaced from their proper positions and thus have a higher energy. In order to keep the total energy as low as possible, the dislocation tries to be as short as possible – it behaves as if it had a *line tension*,  $T$ , like a rubber band. Very roughly, the strains at a dislocation core are of order  $1/2$ ; the stresses are therefore of order  $G/2$  (Chapter 8) so the energy per unit volume of core is  $G/8$ . If we take the core radius to be equal to the atom size  $b$ , its volume, per unit length, is  $\pi b^2$ . The line tension is the energy per unit length (just as a surface tension is an energy per unit area), giving

$$T = \frac{\pi}{8} Gb^2 \approx \frac{Gb^2}{2}, \quad (9.3)$$

where  $G$  is the shear modulus. In absolute terms,  $T$  is small (we should need  $\approx 10^8$  dislocations to hold an apple up) but it is large in relation to the size of a

A horizontal line with arrows at both ends pointing outwards. Below the line, centered, is the equation  $T = \frac{Gb^2}{2}$ .

Fig. 9.13. The line tension in a dislocation.

dislocation, and has an important bearing on the way in which obstacles obstruct the motion of dislocations.

We shall be looking in the next chapter at how we can use our knowledge of how dislocations work and how they behave in order to understand how materials deform plastically, and to help us design stronger materials.

### Further reading

- A. H. Cottrell, *The Mechanical Properties of Matter*, Wiley, 1964, Chap. 9.
- D. Hull, *Introduction to Dislocations*, 2nd edition, Pergamon Press, 1975.
- W. T. Read, Jr., *Dislocations in Crystals*, McGraw Hill, 1953.
- J. P. Hirth and J. Lothe, *Theory of Dislocations*, McGraw Hill, 1968.

# Chapter 10

## Strengthening methods, and plasticity of polycrystals

---

### Introduction

We showed in the last chapter that:

- (a) crystals contain dislocations;
- (b) a shear stress  $\tau$ , applied to the slip plane of a dislocation, exerts a force  $\tau b$  per unit length of the dislocation trying to push it forward;
- (c) when dislocations move, the crystal deforms plastically – that is, it yields.

In this chapter we examine ways of increasing the resistance to motion of a dislocation; it is this which determines the *dislocation yield strength* of a single isolated crystal, of a metal or a ceramic. But bulk engineering materials are aggregates of many crystals, or *grains*. To understand the plasticity of such an aggregate, we have to examine also how the individual crystals interact with each other. This lets us calculate the *polycrystal yield strength* – the quantity that enters engineering design.

### Strengthening mechanisms

A crystal yields when the force  $\tau b$  (per unit length) exceeds  $f$ , the *resistance* (a force per unit length) opposing the motion of a dislocation. This defines the dislocation yield strength

$$\tau_y = \frac{f}{b}. \quad (10.1)$$

Most crystals have a certain *intrinsic* strength, caused by the bonds between the atoms which have to be broken and reformed as the dislocation moves. Covalent bonding, particularly, gives a very large *intrinsic lattice resistance*,  $f$ , per unit length of dislocation. It is this that causes the enormous strength and hardness of diamond, and the carbides, oxides, nitrides and silicates which are used for abrasives and cutting tools. But pure metals are very soft: they have a very low lattice resistance. Then it is useful to increase  $f$  by *solid solution strengthening*, by *precipitate* or *dispersion* strengthening, or by *work-hardening*, or by any combination of the three. Remember, however, that there is an upper limit to the yield strength: it can never exceed the ideal strength (Chapter 9). In practice, only a few materials have strengths that even approach it.

## Solid solution hardening

A good way of hardening a metal is simply to make it impure. Impurities go into solution in a solid metal just as sugar dissolves in tea. A good example is the addition of zinc to copper to make the *alloy* called brass. The zinc atoms replace copper atoms to form a *random substitutional solid solution*. At room temperature Cu will dissolve up to 30% Zn in this way. The Zn atoms are bigger than the Cu atoms, and, in squeezing into the Cu structure, generate stresses. These stresses 'roughen' the slip plane, making it harder for dislocations to move; they increase the resistance  $f$ , and thereby increase the dislocation yield strength,  $\tau_y$  (eqn. (10.1)). If the contribution to  $f$  given by the solid solution is  $f_{ss}$  then  $\tau_y$  is increased by  $f_{ss}/b$ . In a solid solution of concentration  $C$ , the spacing of dissolved atoms on the slip plane (or on any other plane, for that matter) varies as  $C^{-1/2}$ ; and the smaller the spacing, the 'rougher' is the slip plane. As a result,  $\tau_y$  increases about parabolically (i.e. as  $C^2$ ) with solute concentration (Fig. 10.1). Single-phase brass, bronze, and stainless steels, and many other metallic alloys, derive their strength in this way.

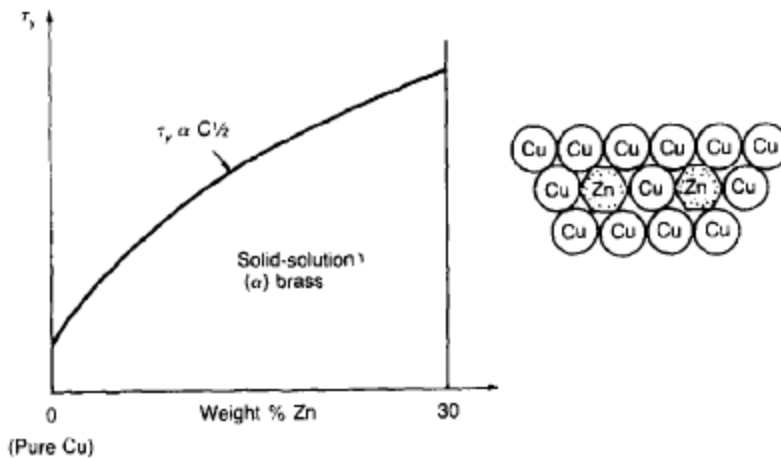


Fig. 10.1. Solid solution hardening.

## Precipitate and dispersion strengthening

If an impurity (copper, say) is dissolved in a metal or ceramic (aluminium, for instance) at a high temperature, and the alloy is cooled to room temperature, the impurity may *precipitate* as small particles, much as sugar will crystallise from a saturated solution when it is cooled. An alloy of Al containing 4% Cu ('Duralumin'), treated in this way, gives very small, closely spaced precipitates of the hard compound  $\text{CuAl}_2$ . Most steels are strengthened by precipitates of carbides, obtained in this way.\*

\*The optimum precipitate is obtained by a more elaborate *heat treatment*: the alloy is *solution heat-treated* (heated to dissolve the impurity), *quenched* (cooled fast to room temperature, usually by dropping it into oil or water) and finally *tempered* or *aged* for a controlled time and at a controlled temperature (to cause the precipitate to form).

Small particles can be introduced into metals or ceramics in other ways. The most obvious is to mix a dispersoid (such as an oxide) into a powdered metal (aluminium and lead are both treated in this way), and then compact and sinter the mixed powders.

Either approach distributes small, hard particles in the path of a moving dislocation. Figure 10.2 shows how they obstruct its motion. The stress  $\tau$  has to push the dislocation between the obstacles. It is like blowing up a balloon in a bird cage: a very large pressure is needed to bulge the balloon between the bars, though once a large enough bulge is formed, it can easily expand further. The *critical configuration* is the semicircular one (Fig. 10.2(c)): here the force  $\tau bL$  on one segment is just balanced by the force  $2T$  due to the line tension, acting on either side of the bulge. The dislocation escapes (and yielding occurs) when

$$\tau_y = \frac{2T}{bL} \quad (10.2)$$

The obstacles thus exert a resistance of  $f_0 = 2T/L$ . Obviously, the greatest hardening is produced by *strong, closely spaced precipitates or dispersions* (Fig. 10.2).

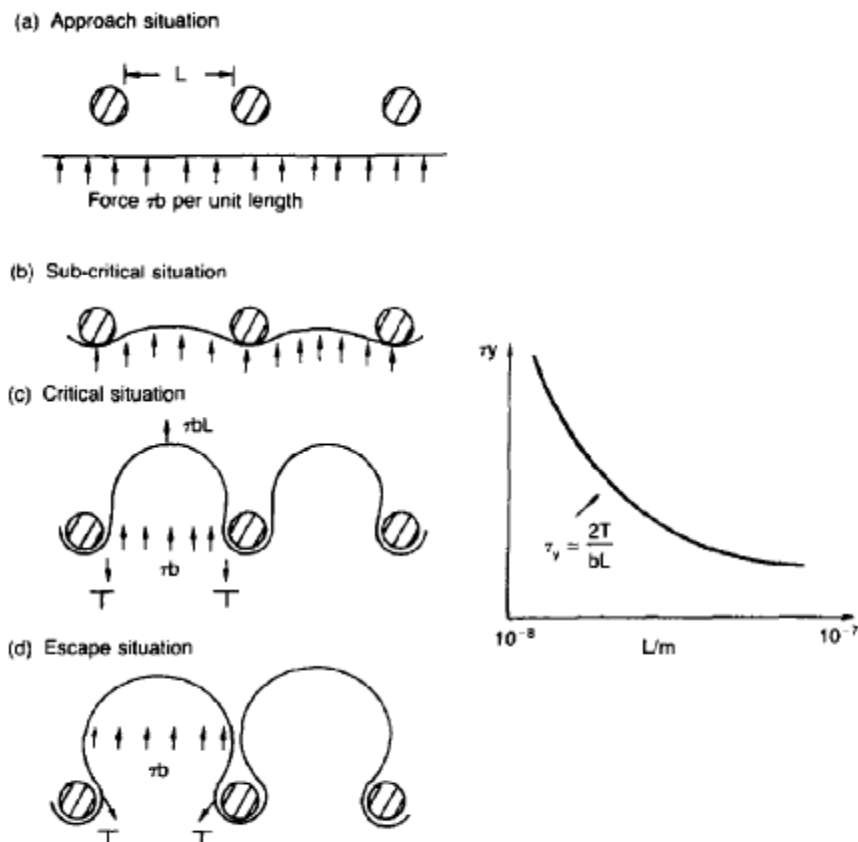


**Fig. 10.2.** How dispersed precipitates help prevent the movement of dislocations, and help prevent plastic flow of materials.

## Work-hardening

When crystals yield, dislocations move through them. Most crystals have several slip planes: the f.c.c. structure, which slips on {111} planes (Chapter 5), has four, for example. Dislocations on these intersecting planes interact, and obstruct each other, and accumulate in the material.

The result is *work-hardening*: the steeply rising stress-strain curve after yield, shown in Chapter 8. All metals and ceramics work-harden. It can be a nuisance: if you want to roll thin sheet, work-hardening quickly raises the yield strength so much that you have to stop and *anneal* the metal (heat it up to remove the accumulated dislocations) before you can go on. But it is also useful: it is a potent strengthening method, which can be added to the other methods to produce strong materials.

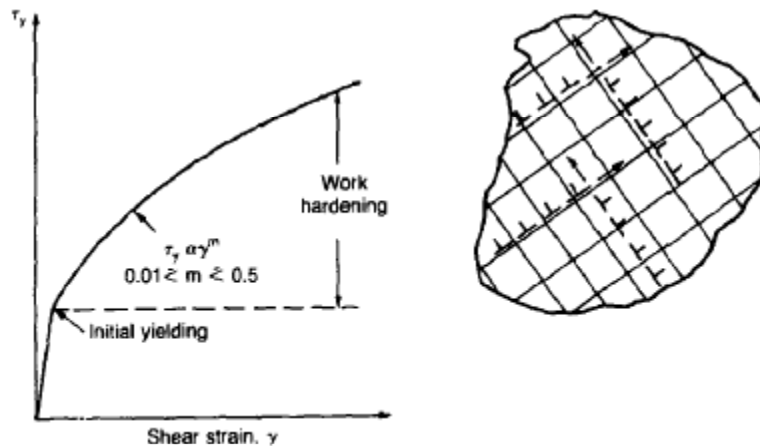


Fig. 10.3. Collision of dislocations leads to work-hardening.

The analysis of work-hardening is difficult. Its contribution  $f_{wh}$  to the total dislocation resistance  $f$  is considerable and increases with strain (Fig. 10.3).

## The dislocation yield strength

It is adequate to assume that the strengthening methods contribute in an additive way to the strength. Then

$$\tau_y = \frac{f_i}{b} + \frac{f_{ss}}{b} + \frac{f_0}{b} + \frac{f_{wh}}{b}. \quad (10.3)$$

Strong materials either have a high intrinsic strength,  $f_i$  (like diamond), or they rely on the superposition of solid solution strengthening  $f_{ss}$ , obstacles  $f_0$  and work-hardening  $f_{wh}$  (like high-tensile steels). But before we can use this information, one problem

remains: we have calculated the yield strength of an *isolated crystal* in *shear*. We want the yield strength of a *polycrystalline aggregate* in *tension*.

## Yield in polycrystals

The crystals, or *grains*, in a polycrystal fit together exactly but their crystal orientations differ (Fig. 10.4). Where they meet, at *grain boundaries*, the crystal structure is disturbed, but the atomic bonds across the boundary are numerous and strong enough that the boundaries do not usually weaken the material.

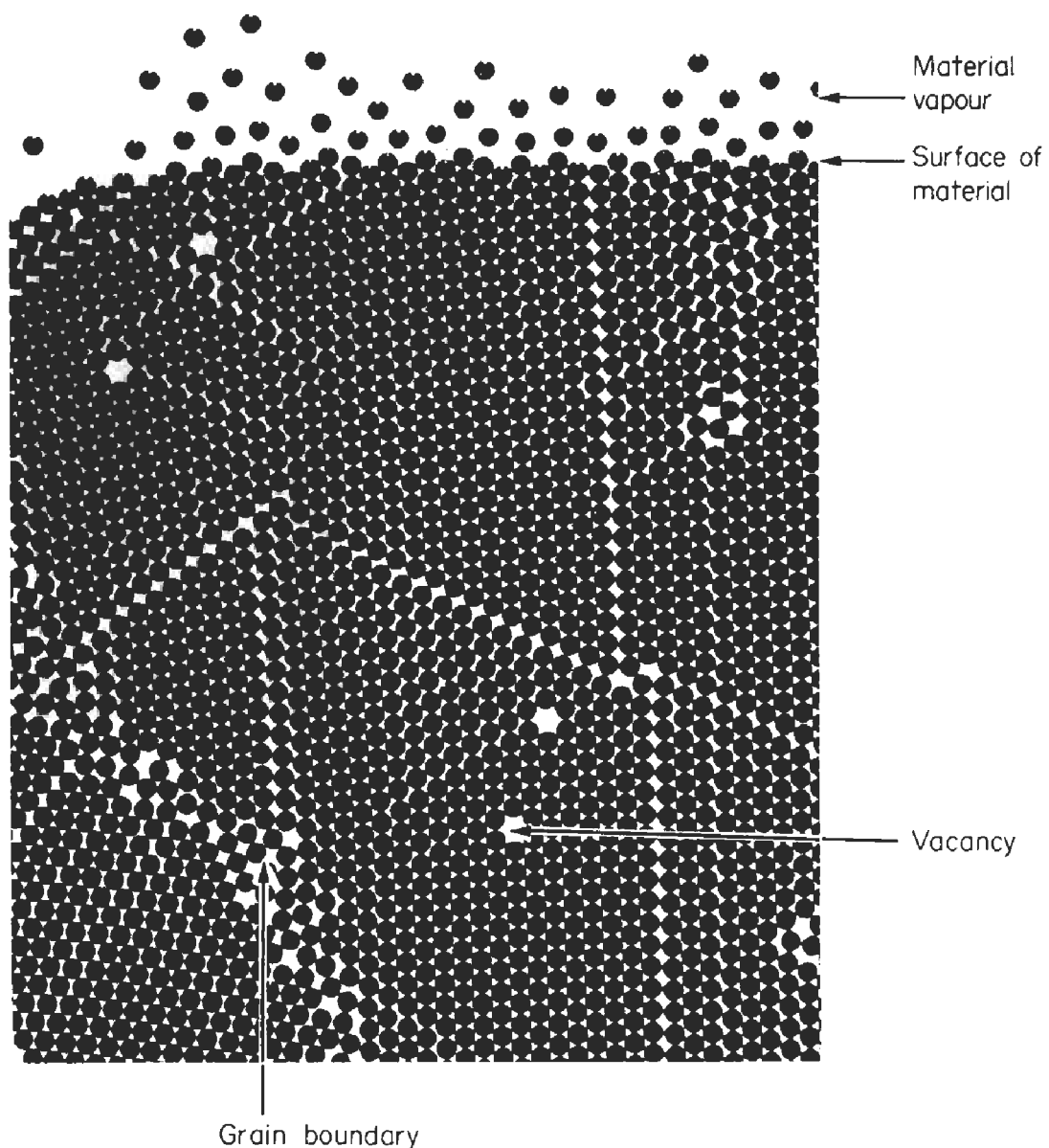


**Fig. 10.4.** Ball bearings can be used to simulate how atoms are packed together in solids. Our photograph shows a ball-bearing model set up to show what the *grain boundaries* look like in a polycrystalline material. The model also shows up another type of defect – the *vacancy* – which is caused by a missing atom.

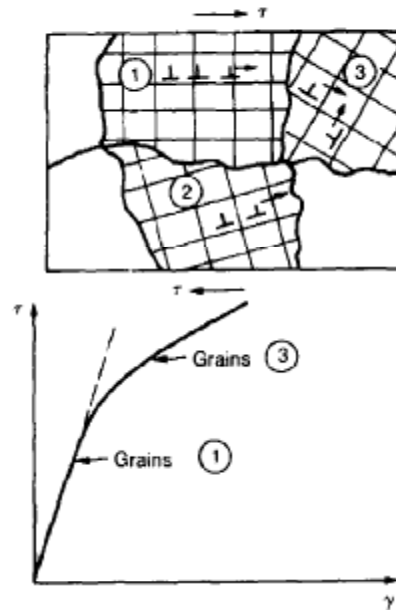


Fig. 10.5. The progressive nature of yielding in a polycrystalline material.

Let us now look at what happens when a polycrystalline component begins to yield (Fig. 10.5). Slip begins in grains where there are slip planes as nearly parallel to  $\tau$  as possible, e.g. grain (1). Slip later spreads to grains like (2) which are not so favourably oriented, and lastly to the worst oriented grains like (3). Yielding does not take place all at once, therefore, and there is no sharp polycrystalline yield point on the stress-strain curve. Further, gross (total) yielding does not occur at the dislocation-yield strength  $\tau_y$  because not all the grains are oriented favourably for yielding. The gross-yield strength is higher, by a factor called the Taylor factor, which is calculated (with difficulty) by averaging the stress over all possible slip planes; it is close to 1.5.

But we want the tensile yield strength,  $\sigma_y$ . A tensile stress  $\sigma$  creates a shear stress in the material that has a maximum value of  $\tau = \sigma/2$ . (We show this in Chapter 11 where we resolve the tensile stress onto planes within the material.) To calculate  $\sigma_y$  from  $\tau_y$  we combine the Taylor factor with the resolution factor to give

$$\sigma_y = 3\tau_y \quad (10.4)$$

$\sigma_y$  is the quantity we want: the yield strength of bulk, polycrystalline solids. It is larger than the dislocation shear strength  $\tau_y$  (by the factor 3) but is proportional to it. So all the statements we have made about increasing  $\tau_y$  apply unchanged to  $\sigma_y$ .

A whole science of alloy design for high strength has grown up in which alloys are blended and heat-treated to achieve maximum  $\tau_y$ . Important components that are strengthened in this way range from lathe tools ('high-speed' steels) to turbine blades ('Nimonic' alloys based on nickel). We shall have more to say about strong solids when

we come to look at how materials are *selected* for a particular job. But first we must return to a discussion of plasticity at the non-atomistic, or continuum, level.

### Further reading

- A. H. Cottrell, *The Mechanical Properties of Matter*, Wiley, 1964, Chap. 9.  
R. W. K. Honeycombe, *The Plastic Deformation of Metals*, Arnold, 1968.

# Chapter 11

## Continuum aspects of plastic flow

---

### Introduction

Plastic flow occurs by shear. Dislocations move when the shear stress on the slip plane exceeds *the dislocation yield strength*  $\tau_y$  of a single crystal. If this is averaged over all grain-orientations and slip planes, it can be related to *the tensile yield strength*  $\sigma_y$  of a polycrystal by  $\sigma_y = 3\tau_y$  (Chapter 10). But in solving problems of plasticity, it is more useful to define *the shear yield strength*  $k$  of a polycrystal. It is equal to  $\sigma_y/2$ , and differs from  $\tau_y$  because it is an average shear-resistance over all orientations of slip plane. When a structure is loaded, the planes on which shear will occur can often be identified or guessed, and the collapse load calculated approximately by requiring that the stress exceed  $k$  on these planes.

In this chapter we show that  $k = \sigma_y/2$ , and use  $k$  to relate the hardness to the yield strength of a solid. We then examine tensile instabilities which appear in the drawing of metals and polymers.

### The onset of yielding and the shear yield strength, $k$

A tensile stress applied to a piece of material will create a shear stress at an angle to the tensile stress. Let us examine the stresses in more detail. Resolving forces in Fig. 11.1 gives the shearing force as

$$F \sin \theta.$$

The area over which this force acts in shear is

$$\frac{A}{\cos \theta}$$

and thus the shear stress,  $\tau$ , is

$$\begin{aligned} \tau &= \frac{F \sin \theta}{A/\cos \theta} = \frac{F}{A} \sin \theta \cos \theta \\ &= \sigma \sin \theta \cos \theta. \end{aligned} \tag{11.1}$$

If we plot this against  $\theta$  as in Fig. 11.2 we find a maximum  $\tau$  at  $\theta = 45^\circ$  to the tensile axis. This means that the *highest value of the shear stress is found at  $45^\circ$  to the tensile axis, and has a value of  $\sigma/2$ .*

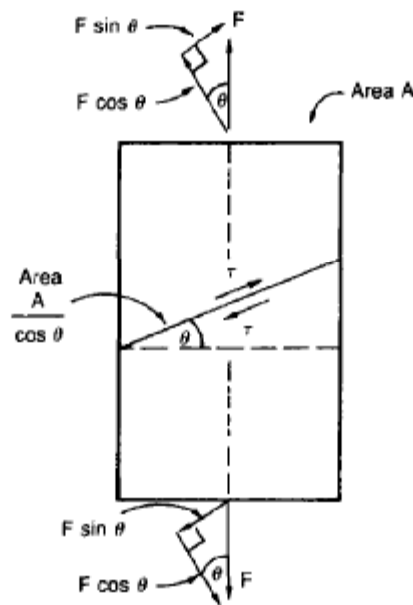


Fig. 11.1. A tensile stress,  $F/A$ , produces a shear stress,  $\tau$ , on an inclined plane in the stressed material.

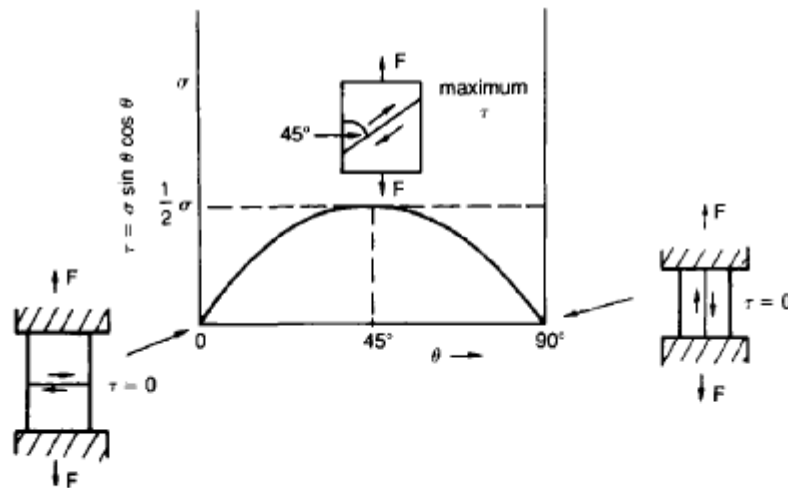


Fig. 11.2. Shear stresses in a material have their maximum value on planes at  $45^\circ$  to the tensile axis.

Now, from what we have said in Chapters 9 and 10, if we are dealing with a single crystal, the crystal will *not* in fact slip on the  $45^\circ$  plane – it will slip on the nearest lattice plane to the  $45^\circ$  plane on which dislocations can glide (Fig. 11.3). In a polycrystal, neighbouring grains each yield on their nearest-to- $45^\circ$  slip planes. On a microscopic scale, slip occurs on a zig-zag path; but the *average* slip path is at  $45^\circ$  to the tensile axis. The shear stress on this plane when yielding occurs is therefore  $\tau = \sigma_y/2$ , and we define this as the shear yield strength  $k$ :

$$k = \sigma_y/2. \tag{11.2}$$

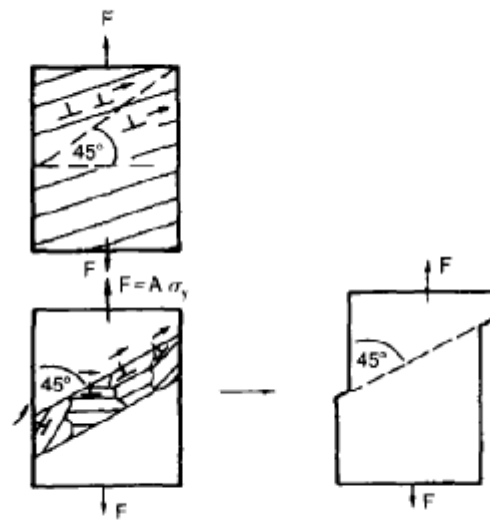


Fig. 11.3. In a polycrystalline material the average slip path is at 45° to the tensile axis.

*Example: Approximate calculation of the hardness of solids.* This concept of shear yielding – where we ignore the details of the grains in our polycrystal and treat the material as a *continuum* – is useful in many respects. For example, we can use it to calculate the loads that would make our material yield for all sorts of quite complicated geometries.

A good example is the problem of the *hardness indenter* that we referred to in the hardness test in Chapter 8. Then, we stated that the hardness

$$H = \frac{F}{A} = 3\sigma_y$$

(with a correction factor for materials that work-harden appreciably – most do). For simplicity, let us assume that our material does not work-harden; so that as the indenter is pushed into the material, the yield strength does not change. Again, for simplicity, we will consider a two-dimensional model. (A real indenter, of course, is three-dimensional, but the result is, for practical purposes, the same.)

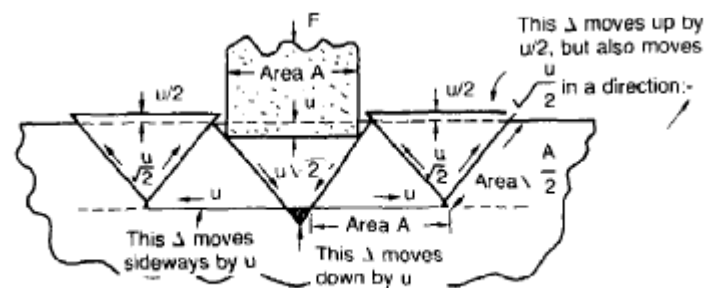


Fig. 11.4. The plastic flow of material under a hardness indenter – a simplified two-dimensional visualisation.

As we press a flat indenter into the material, shear takes place on the  $45^\circ$  planes of maximum shear stress shown in Fig. 11.4, at a value of shear stress equal to  $k$ . By equating the work done by the force  $F$  as the indenter sinks a distance  $u$  to the work done against  $k$  on the shear planes, we get:

$$Fu = 2 \times \frac{Ak}{\sqrt{2}} \times u\sqrt{2} + 2 \times Ak \times u + 4 \times \frac{Ak}{\sqrt{2}} \times \frac{u}{\sqrt{2}}.$$

This simplifies to

$$F = 6Ak$$

from which

$$\frac{F}{A} = 6k = 3\sigma_y.$$

But  $F/A$  is the hardness,  $H$ ; so

$$H = 3\sigma_y. \quad (11.3)$$

(Strictly, shear occurs not just on the shear planes we have drawn, but on a myriad of  $45^\circ$  planes near the indenter. If our assumed geometry for slip is wrong it can be shown rigorously by a theorem called the *upper-bound* theorem that the value we get for  $F$  at yield – the so-called ‘limit’ load – is always on the high side.)

Similar treatments can be used for all sorts of two-dimensional problems: for calculating the plastic collapse load of structures of complex shape, and for analysing metal-working processes like forging, rolling and sheet drawing.

### Plastic instability: necking in tensile loading

We now turn to the other end of the stress–strain curve and explain why, in tensile straining, materials eventually start to *neck*, a name for *plastic instability*. It means that flow becomes localised across one section of the specimen or component, as shown in Fig. 11.5, and (if straining continues) the material fractures there. Plasticine necks readily; chewing gum is very resistant to necking.

We analyse the instability by noting that if a force  $F$  is applied to the end of the specimen of Fig. 11.5, then any section must carry this load. But is it capable of doing so? Suppose one section deforms a little more than the rest, as the figure shows. Its section is less, and the stress in it is therefore larger than elsewhere. If work-hardening has raised the yield strength enough, the reduced section can still carry the force  $F$ ; but if it has not, plastic flow will become localised at the neck and the specimen will fail there. Any section of the specimen can carry a force  $A\sigma$ , where  $A$  is its area, and  $\sigma$  its current strength. If  $A\sigma$  increases with strain, the specimen is

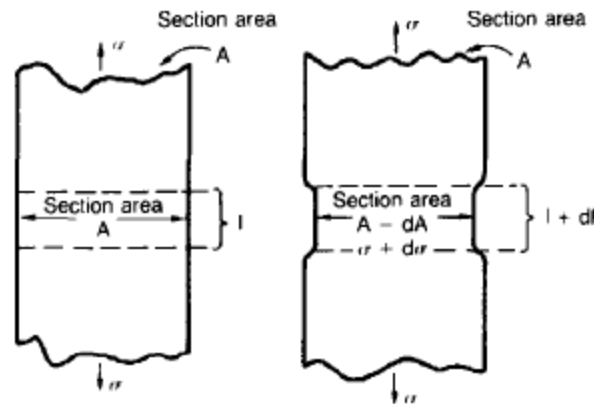


Fig. 11.5. The formation of a neck in a bar of material which is being deformed plastically.

stable. If it decreases, it is unstable and will neck. The critical condition for the start of necking is that

$$A\sigma = F = \text{constant.}$$

Then

$$A d\sigma + \sigma dA = 0$$

or

$$\frac{d\sigma}{\sigma} = -\frac{dA}{A}.$$

But volume is conserved during plastic flow, so

$$-\frac{dA}{A} = \frac{dl}{l} = d\epsilon$$

(prove this by differentiating  $Al = \text{constant}$ ). So

$$\frac{d\sigma}{\sigma} = d\epsilon$$

or

$$\frac{d\sigma}{d\epsilon} = \sigma. \quad (11.4)$$

This equation is given in terms of true stress and true strain. As we said in Chapter 8, tensile data are usually given in terms of nominal stress and strain. From Chapter 8:

$$\sigma = \sigma_n (1 + \epsilon_n),$$

$$\epsilon = \ln(1 + \epsilon_n).$$

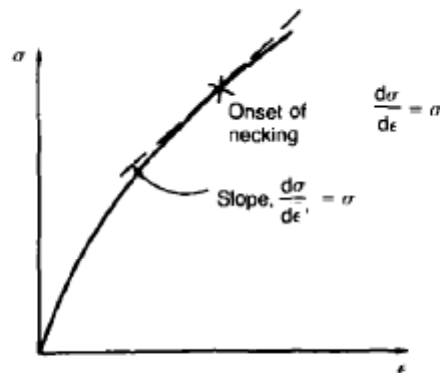


Fig. 11.6. The condition for necking.

If these are differentiated and substituted into the necking equation we get

$$\frac{d\sigma_n}{d\epsilon_n} = 0. \quad (11.5)$$

In other words, on the point of instability, the *nominal* stress–strain curve is at its maximum as we know experimentally from Chapter 8.

To see what is going on physically, it is easier to return to our first condition. At low stress, if we make a little neck, the material in the neck will work-harden and will be able to carry the extra stress it has to stand because of its smaller area; load will therefore be continuous, and the material will be stable. At high stress, the *rate of work-hardening* is less as the true stress–true strain curve shows: i.e. the slope of the  $\sigma/\epsilon$  curve is less. Eventually, we reach a point at which, when we make a neck, the work-hardening is only *just* enough to stand the extra stress. This is the point of necking, with

$$\frac{d\sigma}{d\epsilon} = \sigma.$$

At still higher *true* stress,  $d\sigma/d\epsilon$ , the rate of work-hardening decreases further, becoming insufficient to maintain stability – the extra stress in the neck can no longer be accommodated by the work-hardening produced by making the neck, and the neck grows faster and faster, until final fracture takes place.

#### Consequences of plastic instability

Plastic instability is very important in processes like deep drawing sheet metal to form car bodies, cans, etc. Obviously we must ensure that the materials and press designs are chosen carefully to *avoid* instability.

Mild steel is a good material for deep drawing in the sense that it flows a great deal before necking starts. It can therefore be drawn very deeply without breaking (Fig. 11.7).

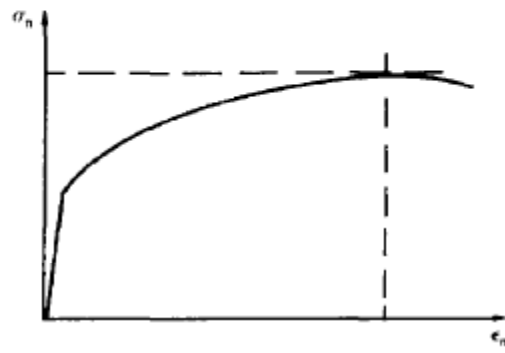


Fig. 11.7. Mild steel can be drawn out a lot before it fails by necking.

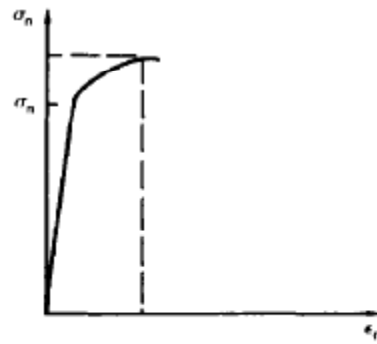


Fig. 11.8. Aluminium alloy quickly necks when it is drawn out.

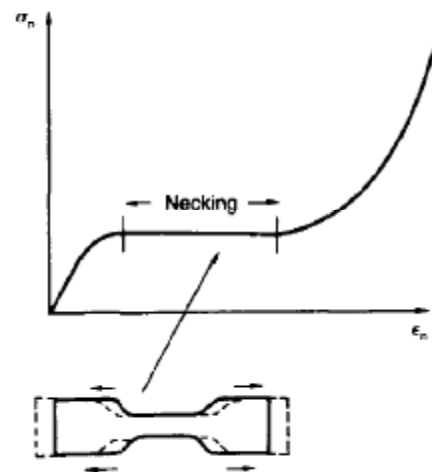


Fig. 11.9. Polythene forms a stable neck when it is drawn out; drawn polythene is very strong.

Aluminium alloy is much less good (Fig. 11.8) – it can only be drawn a little before instabilities form. Pure aluminium is not nearly as bad, but is much too *soft* to use for most applications.

Polythene shows a kind of necking that does *not* lead to fracture. Figure 11.9 shows its  $\sigma_n/\epsilon_n$  curve. At quite low stress

$$\frac{d\sigma_n}{d\epsilon_n}$$

becomes zero and necking begins. However, the neck never becomes *unstable* – it simply grows in length – because at high strain the material work-hardens considerably, and is able to support the increased stress at the reduced cross-section of the neck. This odd behaviour is caused by the lining up of the polymer chains in the neck along the direction of the neck – and for this sort of reason *drawn* (i.e. ‘fully necked’) polymers can be made to be very strong indeed – much stronger than the undrawn polymers.

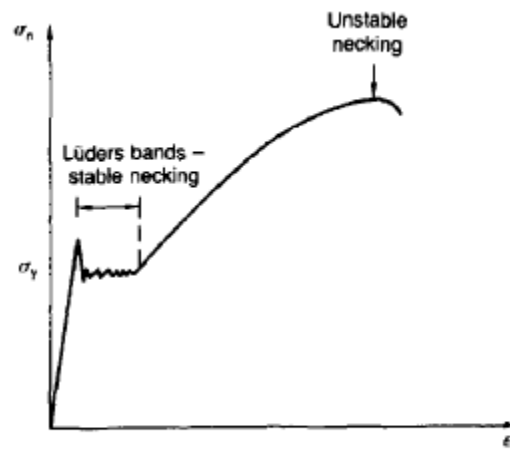


Fig. 11.10. Mild steel often shows both stable and unstable necks.

Finally, mild steel can sometimes show an instability like that of polythene. If the steel is annealed, the stress/strain curve looks like that in Fig. 11.10. A stable neck, called a Lüders Band, forms and propagates (as it did in polythene) without causing fracture because the strong work-hardening of the later part of the stress/strain curve prevents this. Lüders Bands are a problem when sheet steel is pressed because they give lower precision and disfigure the pressing.

### Further reading

- A. H. Cottrell, *The Mechanical Properties of Matter*, Wiley, 1964, Chap. 10.
- C. R. Calladine, *Engineering Plasticity*, Pergamon Press, 1969.
- W. A. Backofen, *Deformation Processing*, Addison-Wesley, 1972.
- R. Hill, *The Mathematical Theory of Plasticity*, Oxford University Press, 1950.

# Chapter 12

## Case studies in yield-limited design

---

### Introduction

We now examine three applications of our understanding of plasticity. The first (material selection for a spring) requires that there be *no plasticity whatever*. The second (material selection for a pressure vessel) typifies plastic design of a large structure. It is unrealistic to expect no plasticity: there will always be some, at bolt holes, loading points, or changes of section. The important thing is that yielding should not spread entirely through any section of the structure – that is, that *plasticity must not become general*. Finally, we examine an instance (the rolling of metal strip) in which yielding is deliberately induced, to give *large-strain plasticity*.

### CASE STUDY 1: ELASTIC DESIGN: MATERIALS FOR SPRINGS

Springs come in many shapes and have many purposes. One thinks of axial springs (a rubber band, for example), leaf springs, helical springs, spiral springs, torsion bars. Regardless of their shape or use, the best materials for a spring of minimum volume is that with the greatest value of  $\sigma_y^2/E$ . Here  $E$  is Young's modulus and  $\sigma_y$  the failure strength of the material of the spring: its yield strength if ductile, its fracture strength or modulus of rupture if brittle. Some materials with high values of this quantity are listed in Table 12.1.

**Table 12.1** Materials for springs

	$E$ (GN m <sup>-2</sup> )	$\sigma_y$ (MN m <sup>-2</sup> )	$\sigma_y^2/E$ (MJ m <sup>-3</sup> )	$\sigma_y/E$
Brass (cold-rolled)	} 120	638	3.38	$5.32 \times 10^{-3}$
Bronze (cold-rolled)		640	3.41	$5.33 \times 10^{-3}$
Phosphor bronze		770	4.94	$6.43 \times 10^{-3}$
Beryllium copper		1380	15.9	$11.5 \times 10^{-3}$
Spring steel	} 200	1300	8.45	$6.5 \times 10^{-3}$
Stainless steel (cold-rolled)		1000	5.0	$5.0 \times 10^{-3}$
Nimonic (high-temp. spring)		614	1.9	$3.08 \times 10^{-3}$

The argument, at its simplest, is as follows. The primary function of a spring is that of storing elastic energy and – when required – releasing it again. The elastic energy stored per unit volume in a block of material stressed uniformly to a stress  $\sigma$  is:

$$U^{el} = \frac{\sigma^2}{2E}$$

It is this that we wish to maximise. The spring will be damaged if the stress  $\sigma$  exceeds the yield stress or failure stress  $\sigma_y$ ; the constraint is  $\sigma \leq \sigma_y$ . So the maximum energy density is

$$U^{el} = \frac{\sigma_y^2}{2E}$$

Torsion bars and leaf springs are less efficient than axial springs because some of the material is not fully loaded: the material at the neutral axis, for instance, is not loaded at all. Consider – since we will need the equations in a moment – the case of a leaf spring.

### The leaf spring

Even leaf springs can take many different forms, but all of them are basically elastic beams loaded in bending. A rectangular section elastic beam, simply supported at both ends, loaded centrally with a force  $F$ , deflects by an amount

$$\delta = \frac{Fl^3}{4Ebt^3} \quad (12.1)$$

ignoring self-weight (Fig. 12.1). Here  $l$  is the length of the beam,  $t$  its thickness,  $b$  its width, and  $E$  is the modulus of the material of which it is made. The elastic energy stored in the spring, per unit volume, is

$$U^{el} = \frac{1}{2} \frac{F\delta}{btl} = \frac{F^2 l^2}{8Eb^2 t^4} \quad (12.2)$$

Figure 12.2 shows that the stress in the beam is zero along the neutral axis at its centre, and is a maximum at the surface, at the mid-point of the beam (because the bending moment is biggest there). The maximum surface stress is given by

$$\sigma = \frac{3Fl}{2bt^2} \quad (12.3)$$



Fig. 12.1. A leaf spring under load.

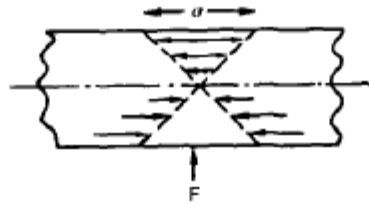


Fig. 12.2. Stresses inside a leaf spring.

Now, to be successful, a spring must not undergo a permanent set during use: it must always 'spring' back. The condition for this is that the maximum stress (eqn. (12.3)) always be less than the yield stress:

$$\frac{3Fl}{2bt^2} < \sigma_y \quad (12.4)$$

Eliminating  $t$  between this and eqn. (12.2) gives

$$U^{(s)} = \frac{1}{18} \left( \frac{\sigma_y^2}{E} \right)$$

This equation says: if in service a spring has to undergo a given deflection,  $\delta$ , under a force  $F$ , the ratio of  $\sigma_y^2/E$  must be high enough to avoid a permanent set. This is why we have listed values of  $\sigma_y^2/E$  in Table 12.1: the best springs are made of materials with high values of this quantity. For this reason spring materials are heavily strengthened (see Chapter 10): by solid solution strengthening plus work-hardening (cold-rolled, single-phase brass and bronze), solid solution and precipitate strengthening (spring steel), and so on. Annealing any spring material removes the work-hardening, and may cause the precipitate to coarsen (increasing the particle spacing), reducing  $\sigma_y$  and making the material useless as a spring.

**Example:** *Springs for a centrifugal clutch.* Suppose that you are asked to select a material for a spring with the following application in mind. A spring-controlled clutch like that shown in Fig. 12.3 is designed to transmit 20 horse power at 800 rpm; the

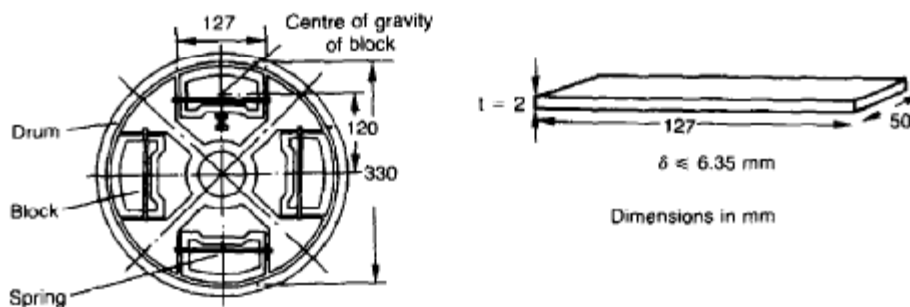


Fig. 12.3. Leaf springs in a centrifugal clutch.

clutch is to begin to pick up load at 600 rpm. The blocks are lined with Ferodo or some other friction material. When properly adjusted, the maximum deflection of the springs is to be 6.35 mm (but the friction pads may wear, and larger deflections may occur; this is a standard problem with springs – almost always, they must withstand occasional extra deflections without losing their sets).

### Mechanics

The force on the spring is

$$F = Mr\omega^2 \quad (12.5)$$

where  $M$  is the mass of the block,  $r$  the distance of the centre of gravity of the block from the centre of rotation, and  $\omega$  the angular velocity. The *net* force the block exerts on the clutch rim at full speed is

$$Mr(\omega_2^2 - \omega_1^2) \quad (12.6)$$

where  $\omega_2$  and  $\omega_1$  correspond to the angular velocities at 800 and 600 rpm (the *net* force must be zero for  $\omega_2 = \omega_1$ , at 600 rpm). The full power transmitted is given by

$$4\mu_s Mr(\omega_2^2 - \omega_1^2) \times \text{distance moved per second by inner rim of clutch at full speed,}$$

i.e.

$$\text{power} = 4\mu_s Mr(\omega_2^2 - \omega_1^2) \times \omega_2 r \quad (12.7)$$

where  $\mu_s$  is the coefficient of static friction.  $r$  is specified by the design (the clutch cannot be too big) and  $\mu_s$  is a constant (partly a property of the clutch-lining material). Both the power and  $\omega_2$  and  $\omega_1$  are specified in eqn. (12.7), so  $M$  is specified also; and finally the maximum force on the spring, too, is determined by the design from  $F = Mr\omega_1^2$ . The requirement that this force deflect the beam by only 6.35 mm with the linings just in contact is what determines the thickness,  $t$ , of the spring via eqn. (12.1) ( $l$  and  $b$  are fixed by the design).

### Metallic materials for the clutch springs

Given the spring dimensions ( $t = 2$  mm,  $b = 50$  mm,  $l = 127$  mm) and given  $\delta \leq 6.35$  mm, all specified by design, which material should we use? Eliminating  $F$  between eqns (12.1) and (12.4) gives

$$\frac{\sigma_y}{E} > \frac{6\delta t}{l^2} = \frac{6 \times 6.35 \times 2}{127 \times 127} = 4.7 \times 10^{-3}. \quad (12.8)$$

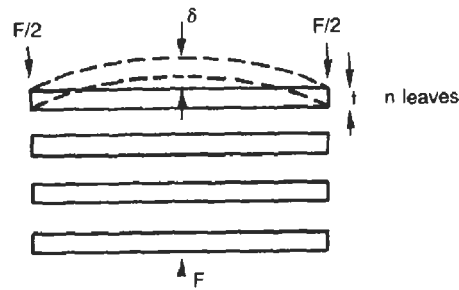


Fig. 12.4. Multi-leaved springs (schematic).

As well as seeking materials with high values of  $\sigma_y^2/E$ , we must also ensure that the material we choose – if it is to have the dimensions specified above and also deflect through 6.35 mm without yielding – meets the criterion of eqn. (12.8).

Table 12.1 shows that spring steel, the cheapest material listed, is adequate for this purpose, but has a worryingly small safety factor to allow for wear of the linings. Only the expensive beryllium–copper alloy, of all the metals shown, would give a significant safety factor ( $\sigma_y/E = 11.5 \times 10^{-3}$ ).

In many designs, the mechanical requirements are such that single springs of the type considered so far would yield even if made from beryllium copper. This commonly arises in the case of suspension springs for vehicles, etc., where both large  $\delta$  ('soft' suspensions) and large  $F$  (good load-bearing capacity) are required. The solution then can be to use multi-leaf springs (Fig. 12.4).  $t$  can be made *small* to give large  $\delta$  without yield according to

$$\left(\frac{\sigma_y}{E}\right) > \frac{6\delta t}{l^2}, \quad (12.9)$$

whilst the lost load-carrying capacity resulting from small  $t$  can be made up by having several leaves combining to support the load.

### Non-metallic materials

Finally, materials other than the metals originally listed in Table 12.1 can make good springs. Glass, or fused silica, with  $\sigma_y/E$  as large as  $58 \times 10^{-3}$  is excellent, *provided* it operates under protected conditions where it cannot be scratched or suffer impact loading (it has long been used for galvanometer suspensions). Nylon is good – provided the forces are low – having  $\sigma_y/E \approx 22 \times 10^{-3}$ , and it is widely used in household appliances and children's toys (you probably brushed your teeth with little nylon springs this morning). Leaf springs for heavy trucks are now being made of CFRP: the value of  $\sigma_y/E$  ( $6 \times 10^{-3}$ ) is similar to that of spring steel, and the weight saving compensates for the higher cost. CFRP is always worth examining where an innovative use of materials might offer advantages.

**CASE STUDY 2: PLASTIC DESIGN: MATERIALS FOR A PRESSURE VESSEL**

We shall now examine material selection for a pressure vessel able to contain a gas at pressure  $p$ , first minimising the *weight*, and then the *cost*. We shall seek a design that will not fail by plastic collapse (i.e. general yield). But we must be cautious: structures can also fail by *fast fracture*, by *fatigue*, and by *corrosion* superimposed on these other modes of failure. We shall discuss these in Chapters 13, 15 and 23. Here we shall assume that plastic collapse is our only problem.

**Pressure vessel of minimum weight**

The body of an aircraft, the hull of a spacecraft, the fuel tank of a rocket: these are examples of pressure vessels which must be as light as possible.

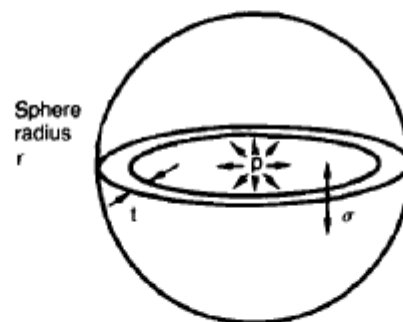


**Fig. 12.5.** Thin-walled spherical pressure vessel.

The stress in the vessel wall (Fig. 12.5) is:

$$\sigma = \frac{pr}{2t}. \quad (12.10)$$

$r$ , the radius of the pressure vessel, is fixed by the design. For safety,  $\sigma \leq \sigma_y/S$ , where  $S$  is the safety factor. The vessel mass is

$$M = 4\pi r^2 t \rho \quad (12.11)$$

so that

$$t = \frac{M}{4\pi r^2 \rho}. \quad (12.12)$$

Substituting for  $t$  in eqn. (12.8) we find that

$$\frac{\sigma_y}{S} \geq \frac{pr}{2} \frac{4\pi r^2 \rho}{M} = \frac{2\pi p r^3 \rho}{M}. \quad (12.13)$$

Table 12.2 Materials for pressure vessels

Material	$\sigma_y$ (MN m <sup>-2</sup> )	$\rho$ (Mg m <sup>-3</sup> )	$\bar{p}$ (UK£ (US\$) tonne <sup>-1</sup> )	$\frac{\rho}{\sigma_y} \times 10^3$	$\frac{\bar{p}\rho}{\sigma_y} \times 10^6$
Reinforced concrete	200	2.5	160 (240)	13	2.1
Alloy steel (pressure-vessel steel)	1000	7.8	500 (750)	7.8	3.9
Mild steel	220	7.8	300 (450)	36	10.8
Aluminium alloy	400	2.7	1100 (1650)	6.8	7.5
Fibreglass	200	1.8	2000 (3000)	9.0	18
CFRP	600	1.5	50,000 (75,000)	2.5	125

From eqn. (12.11) we have, for the mass,

$$M = S2\pi pr^3 \left( \frac{\rho}{\sigma_y} \right) \quad (12.14)$$

so that for the lightest vessel we require the smallest value of  $(\rho/\sigma_y)$ . Table 12.2 gives values of  $\rho/\sigma_y$  for candidate materials.

By far the lightest pressure vessel is that made of CFRP. Aluminium alloy and pressure-vessel steel come next. Reinforced concrete or mild steel results in a very heavy vessel.

#### Pressure vessel of minimum cost

If the cost of the material is  $\bar{p}$  UK£(US\$) tonne<sup>-1</sup> then the material cost of the vessel is

$$\bar{p}M = \text{constant } \bar{p} \left( \frac{\rho}{\sigma_y} \right). \quad (12.15)$$

Thus material costs are minimised by minimising  $\bar{p}(\rho/\sigma_y)$ . Data are given in Table 12.2.

The proper choice of material is now a quite different one. Reinforced concrete is now the best choice – that is why many water towers, and pressure vessels for nuclear reactors, are made of reinforced concrete. After that comes pressure-vessel steel – it offers the best compromise of both price and weight. CFRP is very expensive.

### CASE STUDY 3: LARGE-STRAIN PLASTICITY – ROLLING OF METALS

*Forging, sheet drawing and rolling* are metal-forming processes by which the section of a billet or slab is reduced by compressive plastic deformation. When a slab is rolled (Fig. 12.6) the section is reduced from  $t_1$  to  $t_2$  over a length  $l$  as it passes through the rolls. At first sight, it might appear that there would be no sliding (and thus no friction) between the slab and the rolls, since these move with the slab. But the metal is elongated in the rolling direction, so it speeds up as it passes through the rolls, and

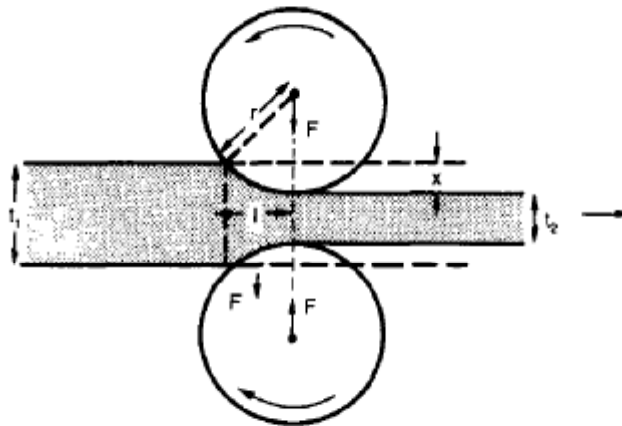


Fig. 12.6. The rolling of metal sheet.

some slipping is inevitable. If the rolls are polished and lubricated (as they are for precision and cold-rolling) the frictional losses are small. We shall ignore them here (though all detailed treatments of rolling include them) and calculate the *rolling torque* for perfectly lubricated rolls.

From the geometry of Fig. 12.6

$$l^2 + (r - x)^2 = r^2$$

or, if  $x = \frac{1}{2}(t_1 - t_2)$  is small (as it almost always is),

$$l = \sqrt{r(t_1 - t_2)}.$$

The rolling force  $F$  must cause the metal to yield over the length  $l$  and width  $w$  (normal to Fig. 12.6). Thus

$$F = \sigma_y w l.$$

If the reaction on the rolls appears halfway along the length marked  $l$ , as shown on the lower roll, the torque is

$$\begin{aligned} T &= \frac{Fl}{2} \\ &= \frac{\sigma_y w l^2}{2}, \end{aligned}$$

giving

$$T = \frac{\sigma_y w r (t_1 - t_2)}{2}. \quad (12.16)$$

The torque required to drive the rolls increases with yield strength  $\sigma_y$ , so hot-rolling (when  $\sigma_y$  is low – see Chapter 17) takes less power than cold-rolling. It obviously increases with the reduction in section ( $t_1 - t_2$ ). And it increases with roll diameter  $2r$ ; this is one of the reasons why small-diameter rolls, often backed by two or more rolls of larger diameter (simply to stop them bending), are used.

Rolling can be analysed in much more detail to include important aspects which we have ignored: friction, the elastic deformation of the rolls, and the constraint of plane strain imposed by the rolling geometry. But this case study gives an idea of why an understanding of plasticity, and the yield strength, is important in forming operations, both for metals and polymers.

### Further reading

- C. R. Calladine, *Engineering Plasticity*, Pergamon Press, 1969.
- R. Hill, *The Mathematical Theory of Plasticity*, Oxford University Press, 1950.
- W. A. Backofen, *Deformation Processing*, Addison-Wesley, 1972.
- M. F. Ashby, *Materials Selection in Mechanical Design*, Pergamon Press, Oxford, 1992.
- M. F. Ashby and D. Cebon, *Case Studies in Materials Selection*, Granta Design, Cambridge, 1996.



## **D. Fast fracture, toughness and fatigue**

---



# Chapter 13

## Fast fracture and toughness

---

### Introduction

Sometimes, structures which were properly designed to avoid both excessive elastic deflection and plastic yielding fail in a catastrophic way by *fast fracture*. Common to these failures – of things like welded ships, welded bridges and gas pipelines and pressure vessels under large internal pressures – is the presence of cracks, often the result of imperfect welding. Fast fracture is caused by the growth – at the speed of sound in the material – of existing cracks that suddenly became unstable. Why do they do this?

### Energy criterion for fast fracture

If you blow up a balloon, energy is stored in it. There is the energy of the compressed gas in the balloon, and there is the elastic energy stored in the rubber membrane itself. As you increase the pressure, the total amount of elastic energy in the system increases.

If we then introduce a flaw into the system, by poking a pin into the inflated balloon, the balloon will explode, and all this energy will be released. The membrane fails by fast fracture, *even though well below its yield strength*. But if we introduce a flaw of the same dimensions into a system with *less* energy in it, as when we poke our pin into a *partially* inflated balloon, the flaw is stable and fast fracture does not occur. Finally, if we blow up the punctured balloon progressively, we eventually reach a pressure at which it suddenly bursts. In other words, we have arrived at a *critical* balloon pressure at which our pin-sized flaw is just unstable, and fast fracture *just* occurs. Why is this?

To make the flaw grow, say by 1 mm, we have to tear the rubber to create 1 mm of new crack surface, and this consumes energy: the tear energy of the rubber per unit area  $\times$  the area of surface torn. If the work done by the gas pressure inside the balloon, plus the release of elastic energy from the membrane itself, is less than this energy the tearing simply cannot take place – it would infringe the laws of thermodynamics.

We can, of course, increase the energy in the system by blowing the balloon up a bit more. The crack or flaw will remain stable (i.e. it will not grow) until the system (balloon plus compressed gas) has stored in it enough energy that, if the crack advances, *more energy is released than is absorbed*. There is, then, a *critical pressure* for fast fracture of a pressure vessel containing a crack or flaw of a given size.

All sorts of accidents (the sudden collapsing of bridges, sudden explosion of steam boilers) have occurred – and still do – due to this effect. In all cases, the critical stress – above which enough energy is available to provide the tearing energy needed to

make the crack advance – was exceeded, taking the designer completely by surprise. But how do we calculate this critical stress?

From what we have said already, we can write down an energy balance which must be met if the crack is to advance, and fast fracture is to occur. Suppose a crack of length  $a$  in a material of thickness  $t$  advances by  $\delta a$ , then we require that: work done by loads  $\geq$  change of elastic energy + energy absorbed at the crack tip, i.e.

$$\delta W \geq \delta U^{el} + G_c t \delta a \quad (13.1)$$

where  $G_c$  is the energy absorbed per unit area of crack (not unit area of new surface), and  $t \delta a$  is the crack area.

$G_c$  is a material property – it is the energy absorbed in making unit area of crack, and we call it the *toughness* (or, sometimes, the ‘critical strain energy release rate’). Its units are energy  $m^{-2}$  or  $J m^{-2}$ . A high toughness means that it is hard to make a crack propagate (as in copper, for which  $G_c \approx 10^6 J m^{-2}$ ). Glass, on the other hand, cracks very easily;  $G_c$  for glass is only  $\approx 10 J m^{-2}$ .

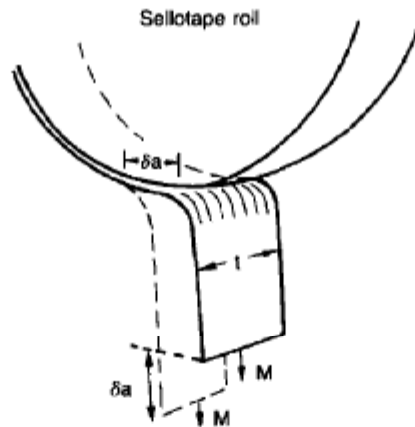


Fig. 13.1. How to determine  $G_c$  for Sellotape adhesive.

This same quantity  $G_c$  measures the strength of adhesives. You can measure it for the adhesive used on sticky tape (like Sellotape) by hanging a weight on a partly peeled length while supporting the roll so that it can freely rotate (hang it on a pencil) as shown in Fig. 13.1. Increase the load to the value  $M$  that just causes rapid peeling (= fast fracture). For this geometry, the quantity  $\delta U^{el}$  is small compared to the work done by  $M$  (the tape has comparatively little ‘give’) and it can be neglected. Then, from our energy formula,

$$\delta W = G_c t \delta a$$

for fast fracture. In our case,

$$Mg \delta a = G_c t \delta a,$$

$$Mg = G_c t,$$

and therefore,

$$G_c = \frac{Mg}{t}.$$

Typically,  $t = 2 \text{ cm}$ ,  $M = 1 \text{ kg}$  and  $g = 10 \text{ m s}^{-2}$ , giving

$$G_c \approx 500 \text{ J m}^{-2}.$$

This is a reasonable value for adhesives, and a value bracketed by the values of  $G_c$  for many polymers.

Naturally, in most cases, we cannot neglect  $\delta U^{\text{el}}$ , and must derive more general relationships. Let us first consider a cracked plate of material loaded so that the displacements at the boundary of the plate are fixed. This is a common mode of loading a material – it occurs frequently in welds between large pieces of steel, for example – and is one which allows us to calculate  $\delta U^{\text{el}}$  quite easily.

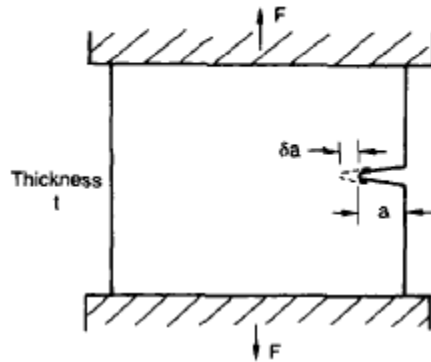


Fig. 13.2. Fast fracture in a fixed plate.

### Fast fracture at fixed displacements

The plate shown in Fig. 13.2 is clamped under tension so that its upper and lower ends are fixed. Since the ends cannot move, the forces acting on them can do no work, and  $\delta W = 0$ . Accordingly, our energy formula gives, for the onset of fast fracture,

$$-\delta U^{\text{el}} = G_c t \delta a. \quad (13.2)$$

Now, as the crack grows into the plate, it allows the material of the plate near the crack to *relax*, so that it becomes less highly stressed, and *loses* elastic energy.  $\delta U^{\text{el}}$  is thus *negative*, so that  $-\delta U^{\text{el}}$  is *positive*, as it must be since  $G_c$  is defined positive. We can estimate  $\delta U^{\text{el}}$  in the way shown in Fig. 13.3.

Let us examine a small cube of material of unit volume inside our plate. Due to the load  $F$  this cube is subjected to a stress  $\sigma$ , producing a strain  $\epsilon$ . Each unit cube therefore

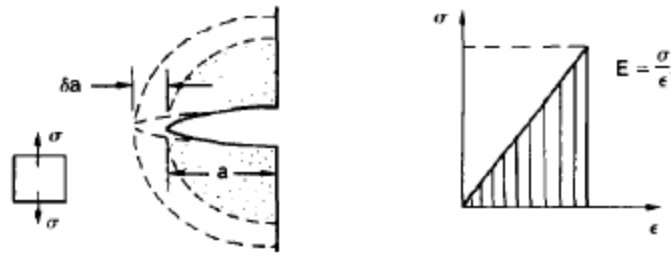


Fig. 13.3. The release of stored strain energy as a crack grows.

has strain energy  $U^{el}$  of  $\frac{1}{2}\sigma\epsilon$ , or  $\sigma^2/2E$ . If we now introduce a crack of length  $a$ , we can consider that the material in the dotted region relaxes (to zero stress) so as to lose all its strain energy. The energy change is

$$U^{el} = -\frac{\sigma^2}{2E} \frac{\pi a^2 t}{2}.$$

As the crack spreads by length  $\delta a$ , we can calculate the appropriate  $\delta U^{el}$  as

$$\delta U^{el} = \frac{dU^{el}}{da} \delta a = -\frac{\sigma^2}{2E} \frac{2\pi a t}{2} \delta a.$$

The critical condition (eqn. (13.2)) then gives

$$\frac{\sigma^2 \pi a}{2E} = G_c$$

at onset of fast fracture.

Actually, our assumption about the way in which the plate material relaxes is obviously rather crude, and a rigorous mathematical solution of the elastic stresses and strains around the crack indicates that our estimate of  $\delta U^{el}$  is too low by exactly a factor of 2. Thus, correctly, we have

$$\frac{\sigma^2 \pi a}{E} = G_c,$$

which reduces to

$$\sigma \sqrt{\pi a} = \sqrt{EG_c} \quad (13.3)$$

at fast fracture.

### Fast fracture at fixed loads

Another, obviously very common way of loading a plate of material, or any other component for that matter, is simply to hang weights on it (fixed loads) (Fig. 13.4). Here the situation is a little more complicated than it was in the case of fixed displacements.

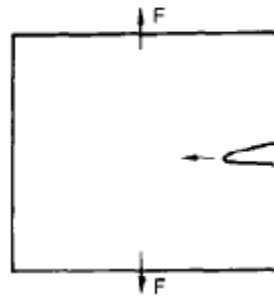


Fig. 13.4. Fast fracture of a dead-loaded plate.

As the crack grows, the plate becomes less *stiff*, and relaxes so that the applied forces move and do work.  $\delta W$  is therefore finite and positive. However,  $\delta U^{el}$  is now positive also (it turns out that some of  $\delta W$  goes into increasing the strain energy of the plate) and our final result for fast fracture is in fact found to be unchanged.

### The fast-fracture condition

Let us now return to our condition for the onset of fast fracture, knowing it to be general\* for engineering structures

$$\sigma\sqrt{\pi a} = \sqrt{EG_c}.$$

The left-hand side of our equation says that *fast fracture will occur when, in a material subjected to a stress  $\sigma$ , a crack reaches some critical size  $a$ : or, alternatively, when material containing cracks of size  $a$  is subjected to some critical stress  $\sigma$ . The right-hand side of our result depends on material properties only;  $E$  is obviously a material constant, and  $G_c$ , the energy required to generate unit area of crack, again must depend only on the basic properties of our material. Thus, the important point about the equation is that *the critical combination of stress and crack length at which fast fracture commences is a material constant.**

The term  $\sigma\sqrt{\pi a}$  crops up so frequently in discussing fast fracture that it is usually abbreviated to a single symbol,  $K$ , having units  $\text{MN m}^{-3/2}$ ; it is called, somewhat unclearly, the *stress intensity factor*. Fast fracture therefore occurs when

$$K = K_c$$

where  $K_c (= \sqrt{EG_c})$  is the *critical stress intensity factor*, more usually called the *fracture toughness*.

To summarise:

$$G_c = \text{toughness (sometimes, critical strain energy release rate). Usual units: } \text{kJ m}^{-2};$$

---

\*But see note at end of this chapter.

$K_c = \sqrt{EG_c}$  = fracture toughness (sometimes: critical stress intensity factor). Usual units:  $\text{MN m}^{-3/2}$ ;

$K = \sigma\sqrt{\pi a}$  = stress intensity factor\*. Usual units:  $\text{MN m}^{-3/2}$ .

Fast fracture occurs when  $K = K_c$ .

### Data for $G_c$ and $K_c$

$K_c$  can be determined experimentally for any material by inserting a crack of known length  $a$  into a piece of the material and loading until fast fracture occurs.  $G_c$  can be derived from the data for  $K_c$  using the relation  $K_c = \sqrt{EG_c}$ . Figures 13.5 and 13.6 and Table 13.1 show experimental data for  $K_c$  and  $G_c$  for a wide range of metals, polymers, ceramics and composites. The values of  $K_c$  and  $G_c$  range considerably, from the least tough materials, like ice and ceramics, to the toughest, like ductile metals; polymers have intermediate toughness,  $G_c$ , but low fracture toughness,  $K_c$  (because their *moduli* are low). However, reinforcing polymers to make *composites* produces materials having good fracture toughnesses. Finally, although most metals are tough at or above room

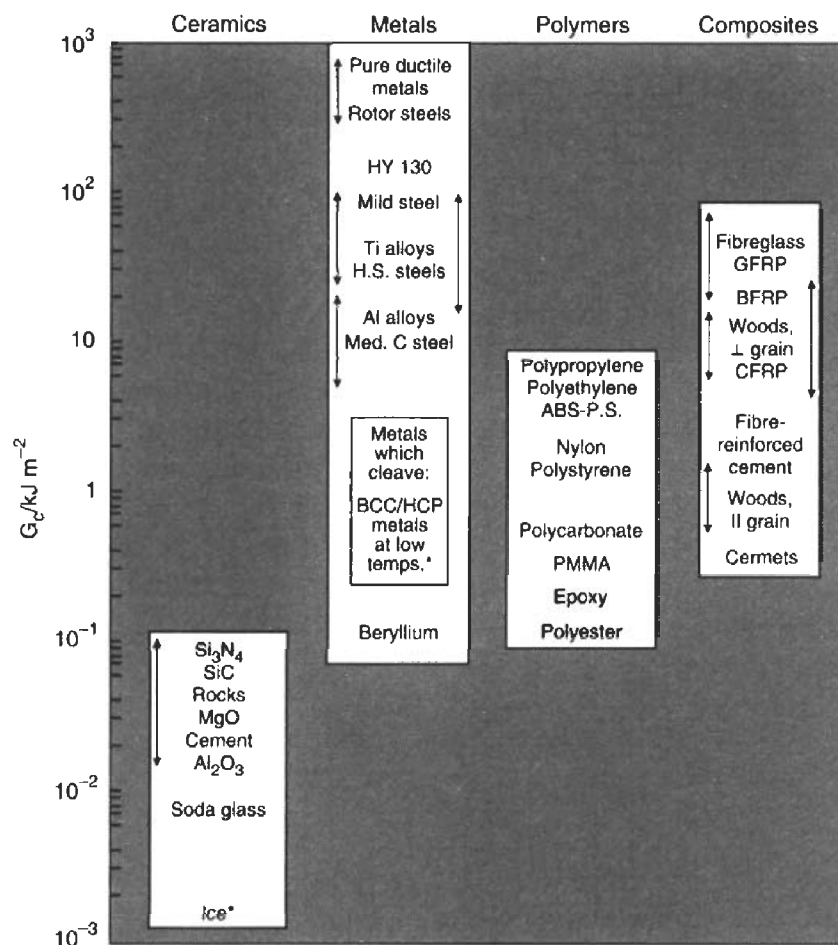


Fig. 13.5. Toughness,  $G_c$  (values at room temperature unless starred).

\*But see note at end of this chapter.

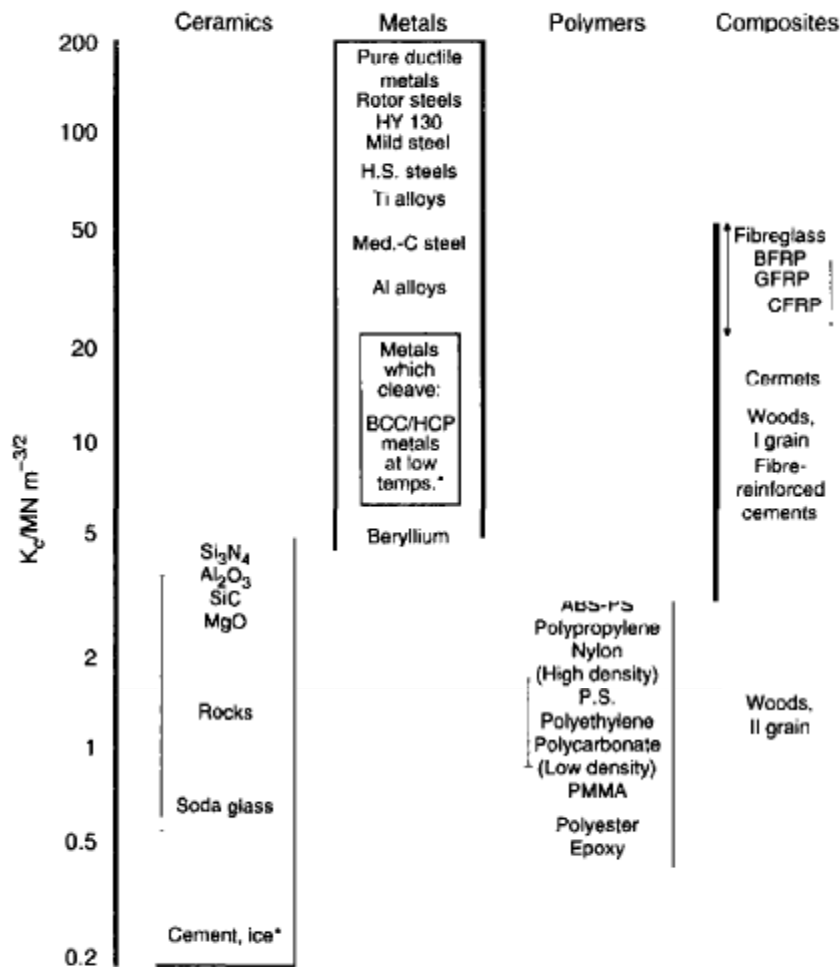


Fig. 13.6. Fracture toughness,  $K_c$  (values at room temperature unless starred).

temperature, when many (e.g. b.c.c. metals like steels, or h.c.p. metals) are cooled sufficiently, they become quite brittle as the data show.

Obviously these figures for toughness and fracture toughness are extremely important – ignorance of such data has led, and can continue to lead, to engineering disasters of the sort we mentioned at the beginning of this chapter. But just how do these large variations between various materials arise? Why is glass so brittle and annealed copper so tough? We shall explain why in Chapter 14.

#### A note on the Stress Intensity, $K$

On pp. 134 and 135 we showed that

$$K = \sigma \sqrt{\pi a} = \sqrt{EG_c}$$

at onset of fast fracture. Strictly speaking, this result is valid only for a crack through the centre of a wide plate of material. In practice, the problems we encounter seldom

**Table 13.1** Toughness,  $G_c$ , and fracture toughness,  $K_{Ic}$ 

Material	$G_c$ (kJ/m <sup>2</sup> )	$K_{Ic}$ (MN/m <sup>3/2</sup> )
Pure ductile metals (e.g. Cu, Ni, Ag, Al)	100–1000	100–350
Rotor steels (A533; Discalloy)	220–240	204–214
Pressure-vessel steels (HY130)	150	170
High-strength steels (HSS)	15–118	50–154
Mild steel	100	140
Titanium alloys (Ti6Al4V)	26–114	55–115
GFRPs	10–100	20–60
Fibreglass (glassfibre epoxy)	40–100	42–60
Aluminium alloys (high strength–low strength)	8–30	23–45
CFRPs	5–30	32–45
Common woods, crack $\perp$ to grain	8–20	11–13
Boron-fibre epoxy	17	46
Medium-carbon steel	13	51
Polypropylene	8	3
Polyethylene (low density)	6–7	1
Polyethylene (high density)	6–7	2
ABS polystyrene	5	4
Nylon	2–4	3
Steel-reinforced cement	0.2–4	10–15
Cast iron	0.2–3	6–20
Polystyrene	2	2
Common woods, crack $\parallel$ to grain	0.5–2	0.5–1
Polycarbonate	0.4–1	1.0–2.6
Cobalt/tungsten carbide cermets	0.3–0.5	14–16
PMMA	0.3–0.4	0.9–1.4
Epoxy	0.1–0.3	0.3–0.5
Granite (Westerly Granite)	0.1	3
Polyester	0.1	0.5
Silicon nitride, Si <sub>3</sub> N <sub>4</sub>	0.1	4–5
Beryllium	0.08	4
Silicon carbide SiC	0.05	3
Magnesia, MgO	0.04	3
Cement/concrete, unreinforced	0.03	0.2
Calcite (marble, limestone)	0.02	0.9
Alumina, Al <sub>2</sub> O <sub>3</sub>	0.02	3–5
Shale (oilshale)	0.02	0.6
Soda glass	0.01	0.7–0.8
Electrical porcelain	0.01	1
Ice	0.003	0.2*

\*Values at room temperature unless starred.

satisfy this geometry, and a numerical correction to  $\sigma\sqrt{\pi a}$  is required to get the strain energy calculation right. In general we write:

$$K = Y \sigma \sqrt{\pi a},$$

where  $Y$  is the numerical correction factor. Values of  $Y$  can be found from tables in standard reference books such as that listed under Further Reading. However,

provided the crack length  $a$  is small compared to the width of the plate  $W$ , it is usually safe to assume that  $Y \approx 1$ .

### Further reading

- R. W. Hertzberg, *Deformation and Fracture Mechanics of Engineering Materials*, 4th edition, 1996.  
B. R. Lawn and T. R. Wilshaw, *Fracture of Brittle Solids*, Cambridge University Press, 1975, Chap. 3.  
J. F. Knott, *Fundamentals of Fracture Mechanics*, Butterworths, 1973, Chap. 4.  
H. Tada, P. Paris and G. Irwin, *The Stress Analysis of Cracks Handbook*, Del Research Corporation, St Louis, 1973 (for Tabulation of Stress Intensities).

# Chapter 14

## Micromechanisms of fast fracture

---

In Chapter 13 we showed that, if a material contains a crack, and is sufficiently stressed, the crack becomes unstable and grows – at up to the speed of sound in the material – to cause catastrophically rapid fracture, or *fast fracture* at a stress less than the yield stress. We were able to quantify this phenomenon and obtained a relationship for the onset of fast fracture

$$\sigma\sqrt{\pi a} = \sqrt{EG_c}$$

or, in more succinct notation,

$$K = K_c \text{ for fast fracture.}$$

It is helpful to compare this with other, similar, ‘failure’ criteria:

$$\sigma = \sigma_y \text{ for yielding,}$$

$$M = M_p \text{ for plastic collapse,}$$

$$P/A = H \text{ for indentation.}$$

(Here  $M$  is the moment and  $M_p$  the fully-plastic moment of, for instance, a beam;  $P/A$  is the indentation pressure and  $H$  the hardness of, for example, armour plating.) The left-hand side of each of these equations describes the *loading conditions*; the right-hand side is a *material property*. When the left-hand side (which increases with load) equals the right-hand side (which is fixed), failure occurs.

Some materials, like glass, have low  $G_c$  and  $K_c$ , and crack easily; ductile metals have high  $G_c$  and  $K_c$  and are very resistant to fast-fracture; polymers have intermediate  $G_c$ , but can be made tougher by making them into composites; and (finally) many metals, when cold, become brittle – that is,  $G_c$  and  $K_c$  fall with temperature. How can we explain these important observations?

### Mechanisms of crack propagation, 1: ductile tearing

Let us first of all look at what happens when we load a cracked piece of a *ductile* metal – in other words, a metal that can flow readily to give large plastic deformations (like pure copper; or mild steel at, or above, room temperature). If we load the material sufficiently, we can get fracture to take place starting from the crack. If you examine the

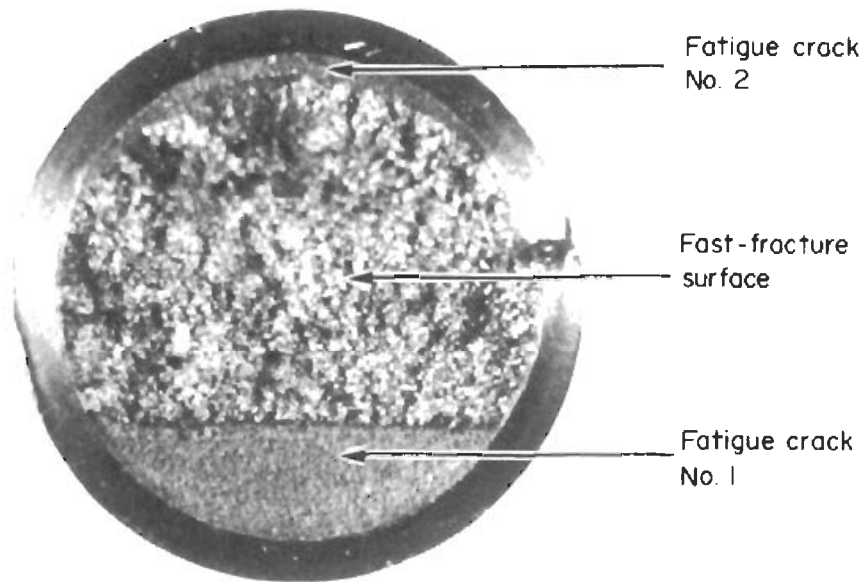


**Fig. 14.1.** Before it broke, this steel bolt held a seat onto its mounting at Milan airport. Whenever someone sat down, the lower part of the cross-section went into tension, causing a crack to grow there by *metal fatigue* (Chapter 15; crack No. 1). When someone got up again, the upper part went into tension, causing fatigue crack No. 2 to grow. Eventually the bolt failed by fast fracture from the larger of the two fatigue cracks. The victim was able to escape with the fractured bolt!

surfaces of the metal after it has fractured (Fig. 14.1) you see that the fracture surface is extremely rough, indicating that a great deal of plastic work has taken place. Let us explain this observation. Whenever a crack is present in a material, the stress close to the crack,  $\sigma_{\text{local}}$ , is greater than the average stress  $\sigma$  applied to the piece of material; the crack has the effect of *concentrating* the stress. Mathematical analysis shows that the local stress ahead of a *sharp* crack in an elastic material is

$$\sigma_{\text{local}} = \sigma + \sigma \sqrt{\frac{a}{2r}}. \quad (14.1)$$

The closer one approaches to the tip of the crack, the higher the local stress becomes, until at some distance  $r_y$  from the tip of the crack the stress reaches the yield stress,  $\sigma_y$ , of the material, and plastic flow occurs (Fig. 14.2). The distance  $r_y$  is easily calculated by setting  $\sigma_{\text{local}} = \sigma_y$  in eqn. (14.1). Assuming  $r_y$  to be small compared to the crack length,  $a$ , the result is

$$\begin{aligned} r_y &= \frac{\sigma^2 a}{2\sigma_y^2} \\ &= \frac{K^2}{2\pi\sigma_y^2}. \end{aligned} \quad (14.2)$$

The crack propagates when  $K$  is equal to  $K_c$ ; the width of the *plastic zone*,  $r_y$ , is then given by eqn. (14.2) with  $K$  replaced by  $K_c$ . Note that the zone of plasticity shrinks

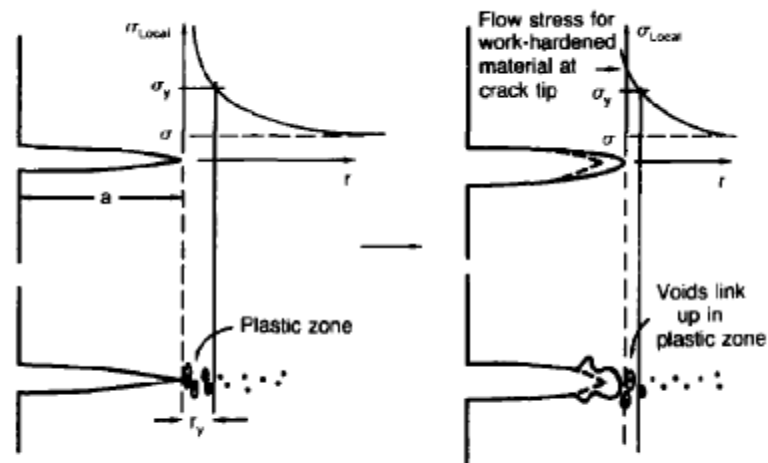


Fig. 14.2. Crack propagation by ductile tearing.

rapidly as  $\sigma_y$  increases: cracks in soft metals have a large plastic zone; cracks in hard ceramics have a small zone, or none at all.

Even when nominally pure, most metals contain tiny *inclusions* (or particles) of chemical compounds formed by reaction between the metal and impurity atoms. Within the plastic zone, plastic flow takes place around these inclusions, leading to elongated cavities, as shown in Fig. 14.2. As plastic flow progresses, these cavities link up, and the crack advances by means of this *ductile tearing*. The plastic flow at the crack tip naturally turns our initially sharp crack into a *blunt crack*, and it turns out from the stress mathematics that this *crack blunting* decreases  $\sigma_{local}$  so that, at the crack tip itself,  $\sigma_{local}$  is just sufficient to keep on plastically deforming the work-hardened material there, as the diagram shows.

The important thing about crack growth by ductile tearing is that *it consumes a lot of energy by plastic flow*; the bigger the plastic zone, the more energy is absorbed. High energy absorption means that  $G_c$  is high, and so is  $K_c$ . This is why ductile metals are so tough. Other materials, too, owe their toughness to this behaviour – plasticine is one, and some polymers also exhibit toughening by processes similar to ductile tearing.

## Mechanisms of crack propagation, 2: cleavage

If you now examine the fracture surface of something like a ceramic, or a glass, you see a very different state of affairs. Instead of a very rough surface, indicating massive local plastic deformation, you see a rather featureless, flat surface suggesting little or no plastic deformation. How is it that cracks in ceramics or glasses can spread without plastic flow taking place? Well, the local stress ahead of the crack tip, given by our formula

$$\sigma_{local} = \sigma + \sigma \sqrt{\frac{a}{2r}},$$

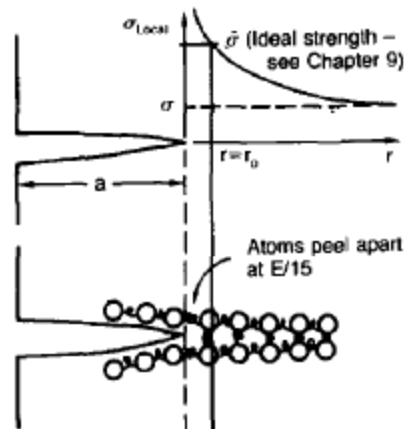


Fig. 14.3. Crack propagation by cleavage.

can clearly approach very high values very near to the crack tip *provided that blunting of our sharp crack tip does not occur*. As we showed in Chapter 8, ceramics and glasses have very high yield strengths, and thus very little plastic deformation takes place at crack tips in these materials. Even allowing for a small degree of crack blunting, the local stress at the crack tip is still in excess of the ideal strength and is thus large enough to literally break apart the interatomic bonds there; the crack then spreads between a pair of atomic planes giving rise to an atomically flat surface by *cleavage*. The energy required simply to break the interatomic bonds is *much* less than that absorbed by ductile tearing in a tough material, and this is why materials like ceramics and glasses are so brittle. It is also why some steels become brittle and fail like glass, at low temperatures – as we shall now explain.

At low temperatures metals having b.c.c. and h.c.p. structures become brittle and fail by cleavage, even though they may be tough at or above room temperature. In fact, only those metals with an f.c.c. structure (like copper, lead, aluminium) remain unaffected by temperature in this way. In metals not having an f.c.c. structure, the motion of dislocations is assisted by the *thermal agitation* of the atoms (we shall talk in more detail about *thermally activated processes* in Chapter 18). At lower temperatures this thermal agitation is less, and the dislocations cannot move as easily as they can at room temperature in response to a stress – the *intrinsic lattice resistance* (Chapter 10) increases. The result is that the yield strength rises, and the plastic zone at the crack tip shrinks until it becomes so small that the fracture mechanism changes from ductile tearing to cleavage. This effect is called the *ductile-to-brittle transition*; for steels it can be as high as  $\approx 0^{\circ}\text{C}$ , depending on the composition of the steel; steel structures like ships, bridges and oil rigs are much more likely to fail in winter than in summer.

A somewhat similar thing happens in many polymers at the *glass-rubber transition* that we mentioned in Chapter 6. Below the transition these polymers are much more brittle than above it, as you can easily demonstrate by cooling a piece of rubber or polyethylene in liquid nitrogen. (Many other polymers, like epoxy resins, have low  $G_c$  values at *all* temperatures simply because they are heavily cross-linked at all temperatures by *covalent bonds* and the material does not flow at the crack tip to cause blunting.)

## Composites, including wood

As Figs. 13.5 and 13.6 show, composites are tougher than ordinary polymers. The low toughness of materials like epoxy resins, or polyester resins, can be enormously increased by reinforcing them with carbon fibre or glass fibre. But why is it that putting a second, equally (or more) brittle material like graphite or glass into a brittle polymer makes a tough composite? The reason is the *fibres act as crack stoppers* (Fig. 14.4).

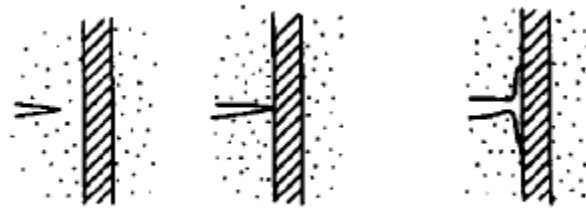


Fig. 14.4. Crack stopping in composites.

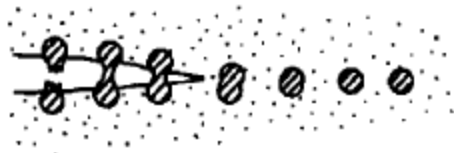


Fig. 14.5. Rubber-toughened polymers.

The sequence in the diagram shows what happens when a crack runs through the brittle matrix towards a fibre. As the crack reaches the fibre, the stress field just ahead of the crack separates the matrix from the fibre over a small region (a process called *debonding*) and the crack is blunted so much that its motion is *arrested*. Naturally, this only works if the crack is running normal to the fibres: wood is very tough across the grain, but can be split easily (meaning that  $G_c$  is low) along it. One of the reasons why fibre composites are so useful in engineering design – in addition to their high *stiffnesses* that we talked about in Chapter 6 – is their high *toughness* produced in this way. Of course, there are other ways of making polymers tough. The addition of small particles ('fillers') of various sorts to polymers can modify their properties considerably. Rubber-toughened polymers (like ABS), for example, derive their toughness from the small rubber particles they contain. A crack intersects and stretches them as shown in Fig. 14.5. The particles act as little springs, clamping the crack shut, and thereby increasing the load needed to make it propagate.

## Avoiding brittle alloys

Let us finally return to the toughnesses of metals and alloys, as these are by far the most important class of materials for highly stressed applications. Even at, or above, room

temperature, when nearly all common pure metals are tough, alloying of these metals with other metals or elements (e.g. with carbon to produce steels) can reduce the toughness. This is because alloying increases the resistance to dislocation motion (Chapter 10), raising the yield strength and causing the plastic zone to shrink. A more marked decrease in toughness can occur if enough impurities are added to make precipitates of chemical *compounds* formed between the metal and the impurities. These compounds can often be very brittle and, if they are present in the shape of extended plates (e.g. sigma-phase in stainless steel; graphite in cast iron), cracks can spread along the plates, leading to brittle fracture. Finally, heat treatments of alloys like steels can produce different *crystal structures* having great hardness (but also therefore great brittleness because crack blunting cannot occur). A good example of such a material is high-carbon steel after quenching into water from bright red heat: it becomes as brittle as glass. Proper heat treatment, following suppliers' specifications, is essential if materials are to have the properties you want. You will see an example of the unexpected results of faulty heat treatment in a Case Study given in Chapter 16.

### Further reading

- B. R. Lawn and T. R. Wilshaw, *Fracture of Brittle Solids*, Cambridge University Press, 1975, Chaps. 6 and 7.  
J. F. Knott, *Fundamentals of Fracture Mechanics*, Butterworths, 1973, Chap. 8.

# Chapter 15

## Fatigue failure

---

### Introduction

In the last two chapters we examined the conditions under which a crack was stable, and would not grow, and the condition

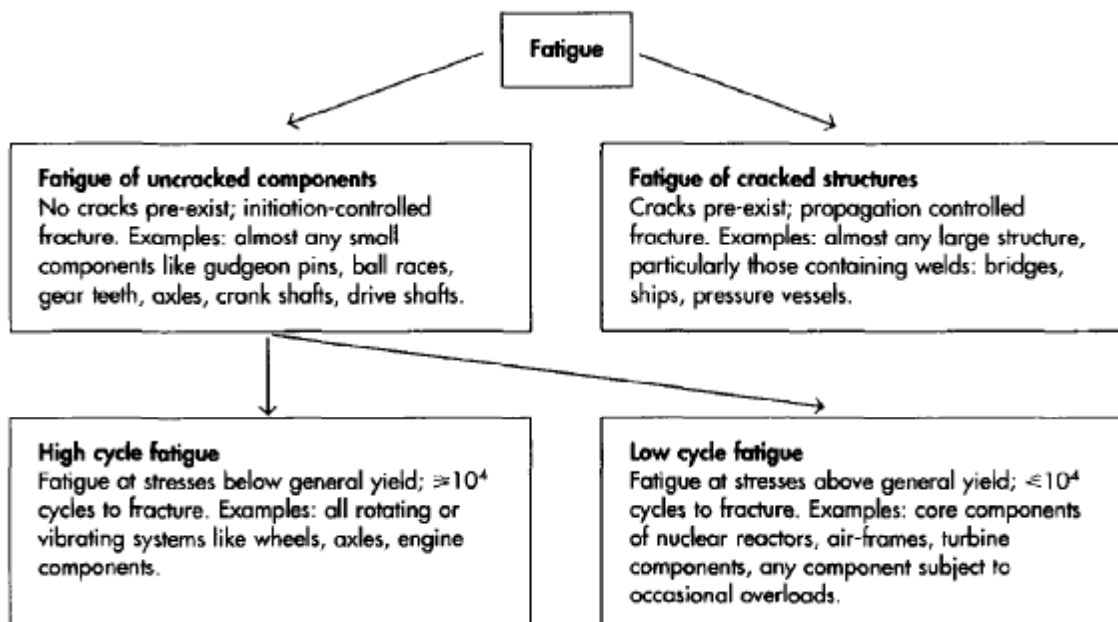
$$K = K_c$$

under which it would propagate catastrophically by fast fracture. If we know the maximum size of crack in the structure we can then choose a working load at which fast fracture will not occur.

But cracks can form, and grow slowly, at loads lower than this, if either the stress is cycled or if the environment surrounding the structure is corrosive (most are). The first process of slow crack growth – *fatigue* – is the subject of this chapter. The second – *corrosion* – is discussed later, in Chapters 21 to 24.

More formally: *if a component or structure is subjected to repeated stress cycles, like the loading on the connecting rod of a petrol engine or on the wings of an aircraft – it may*

Table 15.1



fail at stresses well below the tensile strength,  $\sigma_{ts}$ , and often below the yield strength,  $\sigma_y$ , of the material. The processes leading to this failure are termed 'fatigue'. When the clip of your pen breaks, when the pedals fall off your bicycle, when the handle of the refrigerator comes away in your hand, it is usually fatigue which is responsible.

We distinguish three categories of fatigue (Table 15.1).

### Fatigue behaviour of uncracked components

Tests are carried out by cycling the material either in tension (compression) or in rotating bending (Fig. 15.1). The stress, in general, varies sinusoidally with time,

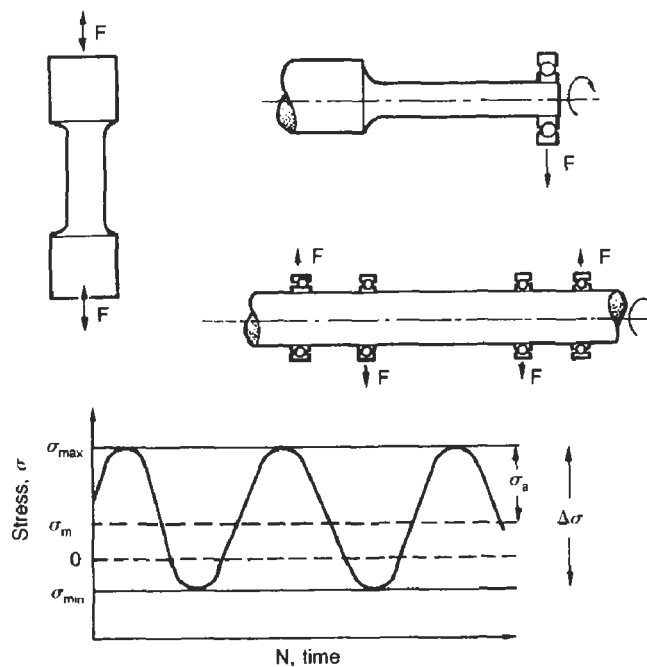


Fig. 15.1. Fatigue testing.

though modern servo-hydraulic testing machines allow complete control of the wave shape.

We define:

$$\Delta\sigma = \sigma_{\max} - \sigma_{\min}; \quad \sigma_m = \frac{\sigma_{\max} + \sigma_{\min}}{2}; \quad \sigma_a = \frac{\sigma_{\max} - \sigma_{\min}}{2}$$

where  $N$  = number of fatigue cycles and  $N_f$  = number of cycles to failure. We will consider fatigue under zero mean stress ( $\sigma_m = 0$ ) first, and later generalise the results to non-zero mean stress.

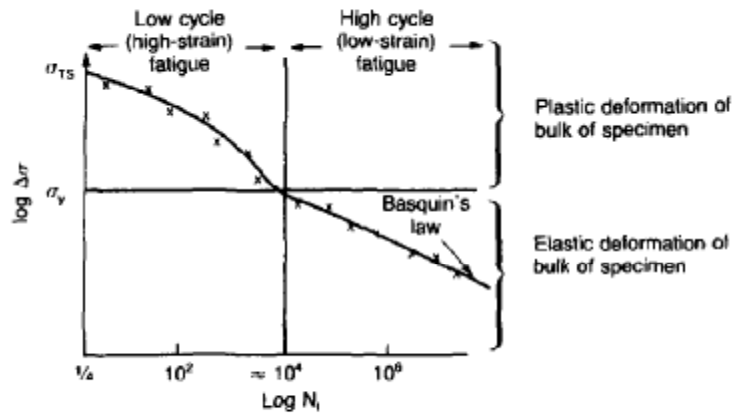


Fig. 15.2. Initiation-controlled high-cycle fatigue – Basquin’s Law.

For *high-cycle fatigue of uncracked components*, where neither  $\sigma_{max}$  nor  $|\sigma_{min}|$  are above the yield stress, it is found empirically that the experimental data can be fitted to an equation of form

$$\Delta\sigma N_f^a = C_1 \tag{15.1}$$

This relationship is called *Basquin’s Law*. Here,  $a$  is a constant (between  $\frac{1}{8}$  and  $\frac{1}{15}$  for most materials) and  $C_1$  is a constant also.

For *low-cycle fatigue of un-cracked components* where  $\sigma_{max}$  or  $|\sigma_{min}|$  are above  $\sigma_y$  Basquin’s Law no longer holds, as Fig. 15.2 shows. But a linear plot is obtained if the plastic strain range  $\Delta\epsilon^{Pl}$ , defined in Fig. 15.3, is plotted, on logarithmic scales, against the cycles to failure,  $N_f$  (Fig. 15.4). This result is known as the *Coffin–Manson Law*:

$$\Delta\epsilon^{Pl} N_f^b = C_2 \tag{15.2}$$

where  $b$  (0.5 to 0.6) and  $C_2$  are constants.

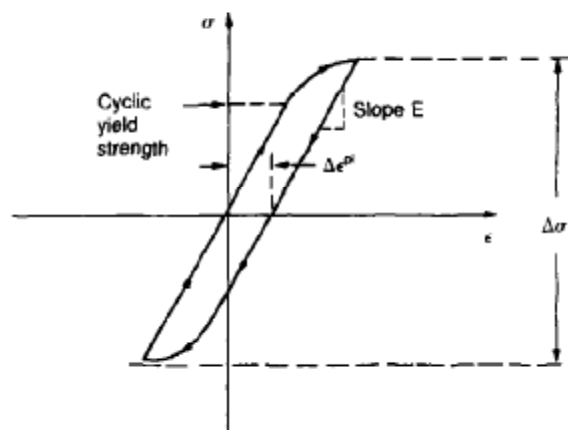


Fig. 15.3. The plastic strain range,  $\Delta\epsilon^{Pl}$ , in low-cycle fatigue.

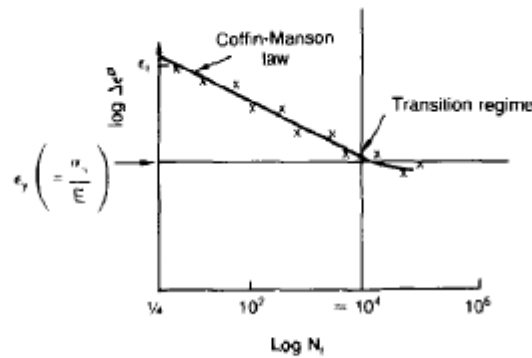


Fig. 15.4. Initiation-controlled low-cycle fatigue – the Coffin–Manson Law.

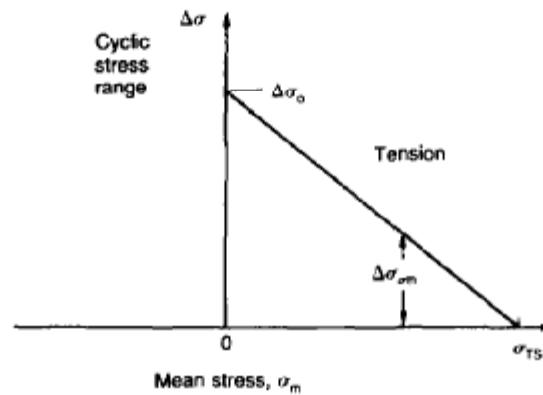


Fig. 15.5. Goodman’s Rule – the effect of a tensile mean stress on initiation-controlled fatigue.

These two laws (given data for  $a, b, C_1$  and  $C_2$ ) adequately describe the fatigue failure of unnotched components, cycled at constant amplitude about a mean stress of zero. What do we do when  $\Delta\sigma$ , and  $\sigma_m$ , vary?

When material is subjected to a mean tensile stress (i.e.  $\sigma_m > 0$ ) the stress range must be decreased to preserve the same  $N_f$  according to *Goodman’s Rule* (Fig. 15.5)

$$\Delta\sigma_{\sigma_m} = \Delta\sigma_0 \left( 1 - \frac{\sigma_m}{\sigma_{TS}} \right). \tag{15.3}$$

(Here  $\Delta\sigma_0$  is the cyclic stress range for failure in  $N_f$  cycles under zero mean stress, and  $\Delta\sigma_{\sigma_m}$  is the same thing for a mean stress of  $\sigma_m$ .) Goodman’s Rule is empirical, and does not always work – then tests simulating service conditions must be carried out, and the results used for the final design. But preliminary designs are usually based on this rule.

When, in addition,  $\Delta\sigma$  varies during the lifetime of a component, the approach adopted is to sum the damage according to *Miner’s Rule* of *cumulative damage*:

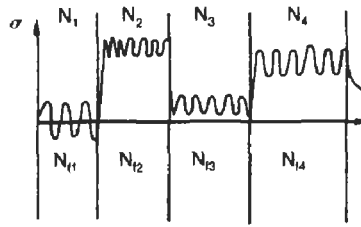


Fig. 15.6. Summing damage due to initiation-controlled fatigue.

$$\sum_i \frac{N_i}{N_{fi}} = 1. \quad (15.4)$$

Here  $N_{fi}$  is the number of cycles to fracture under the stress cycle in region  $i$ , and  $N_i/N_{fi}$  is the fraction of the lifetime used up after  $N_i$  cycles in that region. Failure occurs when the sum of the fractions is unity (eqn. (15.4)). This rule, too, is an empirical one. It is widely used in design against fatigue failure; but if the component is a critical one, Miner's Rule should be checked by tests simulating service conditions.

### Fatigue behaviour of cracked components

Large structures – particularly welded structures like bridges, ships, oil rigs, nuclear pressure vessels – always contain cracks. All we can be sure of is that the initial length of these cracks is less than a given length – the length we can reasonably detect when we check or examine the structure. To assess the safe life of the structure we need to know how long (for how many cycles) the structure can last before one of these cracks grows to a length at which it propagates catastrophically.

Data on fatigue crack propagation are gathered by cyclically loading specimens containing a sharp crack like that shown in Fig. 15.7. We define

$$\Delta K = K_{\max} - K_{\min} = \Delta\sigma\sqrt{\pi a}$$

The cyclic stress intensity  $\Delta K$  increases with time (at constant load) because the crack grows in tension. It is found that the crack growth per cycle,  $da/dN$ , increases with  $\Delta K$  in the way shown in Fig. 15.8.

In the steady-state régime, the crack growth rate is described by

$$\frac{da}{dN} = A\Delta K^m \quad (15.5)$$

where  $A$  and  $m$  are material constants. Obviously, if  $a_0$  (the initial crack length) is given, and the final crack length ( $a_f$ ) at which the crack becomes unstable and runs rapidly is

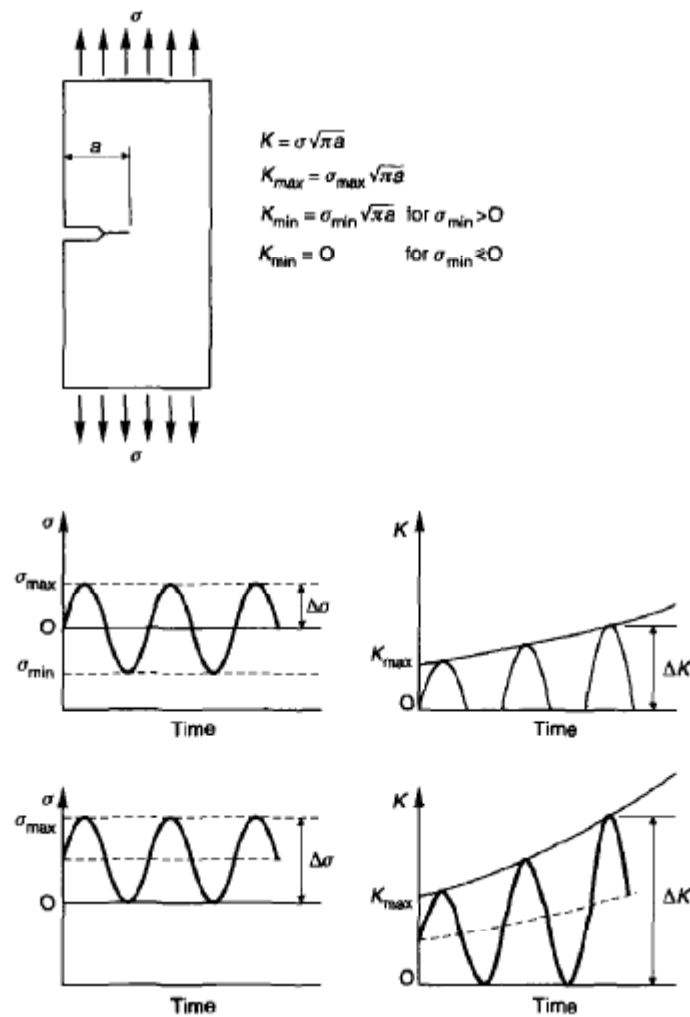


Fig. 15.7. Fatigue-crack growth in pre-cracked components.

known or can be calculated, then the safe number of cycles can be estimated by integrating the equation

$$N_f = \int_0^{N_f} dN = \int_{a_0}^{a_f} \frac{da}{A(\Delta K)^m} \quad (15.6)$$

remembering that  $\Delta K = \Delta\sigma \sqrt{\pi a}$ . Case Study 3 of Chapter 16 gives a worked example of this method of estimating fatigue life.

### Fatigue mechanisms

Cracks grow in the way shown in Fig. 15.9. In a pure metal or polymer (left-hand diagram), the tensile stress produces a plastic zone (Chapter 14) which makes the crack

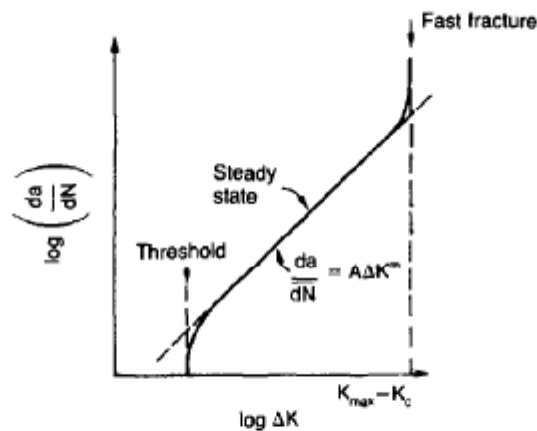


Fig. 15.8. Fatigue crack-growth rates for pre-cracked material.

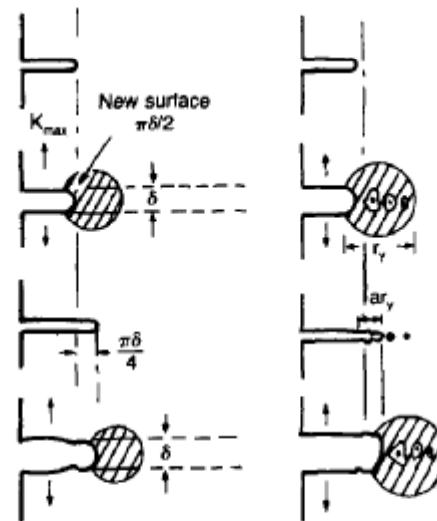


Fig. 15.9. How fatigue cracks grow.

tip stretch open by the amount  $\delta$ , creating new surface there. As the stress is removed the crack closes and the new surface folds forward, extending the crack (roughly, by  $\delta$ ). On the next cycle the same thing happens again, and the crack inches forward, roughly at  $da/dN \approx \delta$ . Note that the crack cannot grow when the stress is compressive because the crack faces come into contact and carry the load (crack closure).

We mentioned in Chapter 14 that real engineering alloys always have little inclusions in them. Then (right-hand diagram of Fig. 15.9), within the plastic zone, holes form and link with each other, and with the crack tip. The crack now advances a little faster than before, aided by the holes.

In *pre-cracked structures* these processes determine the fatigue life. In uncracked components subject to *low-cycle fatigue*, the general plasticity quickly roughens the

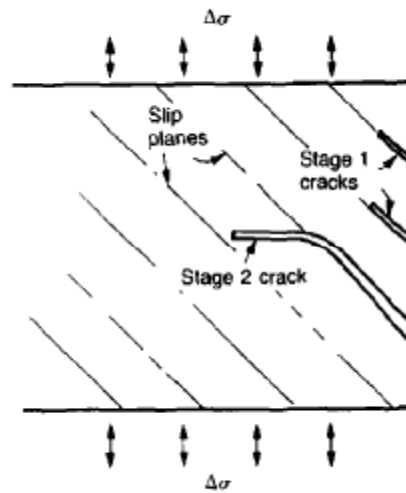


Fig. 15.10. How cracks form in low-cycle fatigue. Once formed, they grow as shown in Fig. 15.9.

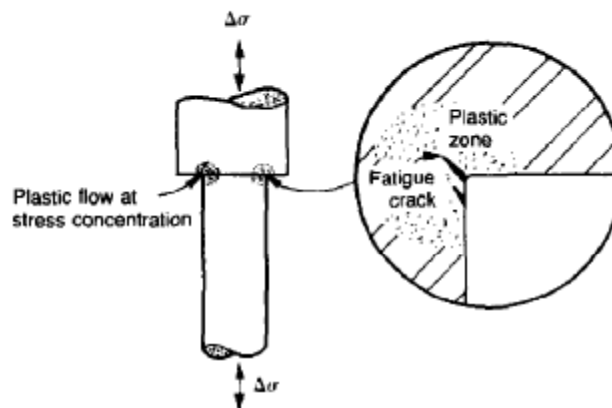


Fig. 15.11. How cracks form in high-cycle fatigue.

surface, and a crack forms there, propagating first along a slip plane ('Stage 1' crack) and then, by the mechanism we have described, normal to the tensile axis (Fig. 15.10).

High-cycle fatigue is different. When the stress is below general yield, almost all of the life is taken up in initiating a crack. Although there is no *general* plasticity, there is *local* plasticity wherever a notch or scratch or change of section concentrates stress. A crack ultimately initiates in the zone of one of these stress concentrations (Fig. 15.11) and propagates, slowly at first, and then faster, until the component fails. For this reason, sudden changes of section or scratches are very dangerous in high-cycle fatigue, often reducing the fatigue life by orders of magnitude.

### Further reading

- R. W. Hertzberg, *Deformation and Fracture Mechanics of Engineering Materials*, 4th edition, Wiley, 1996.
- J. F. Knott, *Fundamentals of Fracture Mechanics*, Butterworths, 1973, Chap. 9.
- T. V. Duggan and J. Byrne, *Fatigue as a Design Criterion*, Macmillan, 1977.

## Chapter 16

# Case studies in fast fracture and fatigue failure

### Introduction

In this third set of Case Studies we examine three instances in which failure by crack-propagation was, or could have become, a problem. The first is the analysis of an ammonia tank that failed by fast fracture. The second concerns a common problem: the checking, for safety reasons, of cylinders designed to hold gas at high pressure. The last is a fatigue problem: the safe life of a reciprocating engine known to contain a large crack.

### CASE STUDY 1: FAST FRACTURE OF AN AMMONIA TANK

Figure 16.1 shows part of a steel tank which came from a road tank vehicle. The tank consisted of a cylindrical shell about 6 m long. A hemispherical cap was welded to each end of the shell with a circumferential weld. The tank was used to transport liquid ammonia. In order to contain the liquid ammonia the pressure had to be equal to the saturation pressure (the pressure at which a mixture of liquid and vapour is in equilibrium). The saturation pressure increases rapidly with temperature: at 20°C the absolute pressure is 8.57 bar; at 50°C it is 20.33 bar. The gauge pressure at 50°C is 19.33 bar, or  $1.9 \text{ MN m}^{-2}$ . Because of this the tank had to function as a pressure vessel. The maximum operating pressure was  $2.07 \text{ MN m}^{-2}$  gauge. This allowed the tank to be used safely to 50°C, above the maximum temperature expected in even a hot climate.

While liquid was being unloaded from the tank a fast fracture occurred in one of the circumferential welds and the cap was blown off the end of the shell. In order to decant

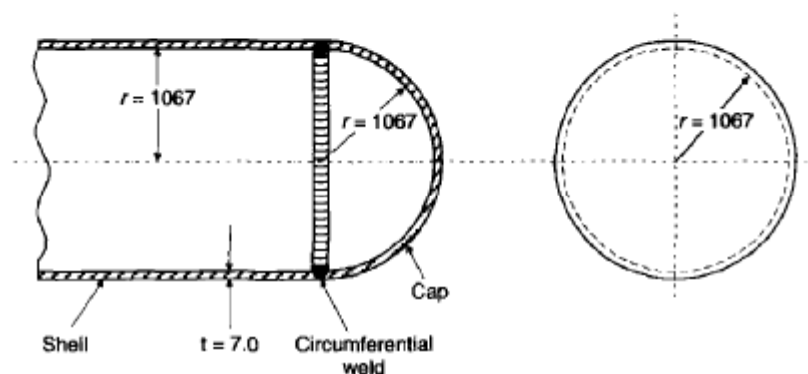


Fig. 16.1. The weld between the shell and the end cap of the pressure vessel. Dimensions in mm.

the liquid the space above the liquid had been pressurised with ammonia gas using a compressor. The normal operating pressure of the compressor was  $1.83 \text{ MN m}^{-2}$ ; the maximum pressure (set by a safety valve) was  $2.07 \text{ MN m}^{-2}$ . One can imagine the effect on nearby people of this explosive discharge of a large volume of highly toxic vapour.

#### Details of the failure

The geometry of the failure is shown in Fig. 16.2. The initial crack, 2.5 mm deep, had formed in the heat-affected zone between the shell and the circumferential weld. The defect went some way around the circumference of the vessel. The cracking was intergranular, and had occurred by a process called stress corrosion cracking (see Chapter 23). The final fast fracture occurred by transgranular cleavage (see Chapter 14). This indicates that the heat-affected zone must have had a very low fracture toughness. In this case study we predict the critical crack size for fast fracture using the fast fracture equation.

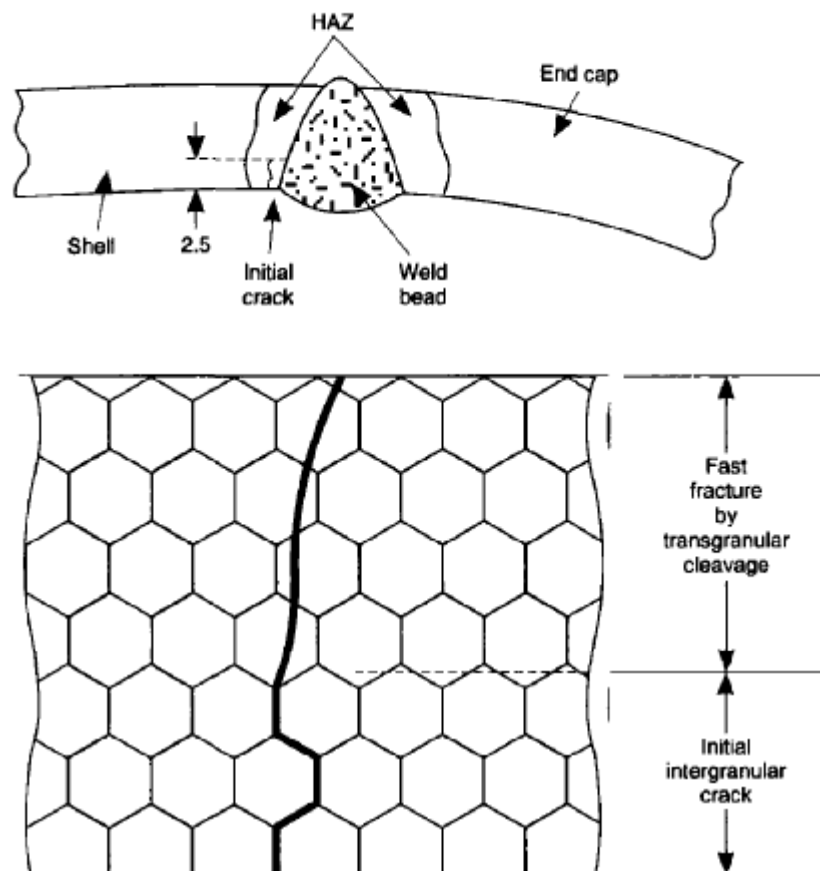


Fig. 16.2. The geometry of the failure. Dimensions in mm.

### Material properties

The tank was made from high-strength low-alloy steel with a yield strength of  $712 \text{ MN m}^{-2}$  and a fracture toughness of  $80 \text{ MN m}^{-3/2}$ . The heat from the welding process had altered the structure of the steel in the heat-affected zone to give a much greater yield strength ( $940 \text{ MN m}^{-2}$ ) but a much lower fracture toughness ( $39 \text{ MN m}^{-3/2}$ ).

### Calculation of critical stress for fast fracture

The longitudinal stress  $\sigma$  in the wall of a cylindrical pressure vessel containing gas at pressure  $p$  is given by

$$\sigma = \frac{pr}{2t},$$

provided that the wall is thin ( $t \ll r$ ).  $p = 1.83 \text{ MN m}^{-2}$ ,  $r = 1067 \text{ mm}$  and  $t = 7 \text{ mm}$ , so  $\sigma = 140 \text{ MN m}^{-2}$ . The fast fracture equation is

$$Y\sigma\sqrt{\pi a} = K_c.$$

Because the crack penetrates a long way into the wall of the vessel, it is necessary to take into account the correction factor  $Y$  (see Chapter 13). Figure 16.3 shows that  $Y = 1.92$  for our crack. The critical stress for fast fracture is given by

$$\sigma = \frac{K_c}{Y\sqrt{\pi a}} = \frac{39}{1.92\sqrt{\pi \cdot 0.0025}} = 229 \text{ MN m}^{-2}.$$

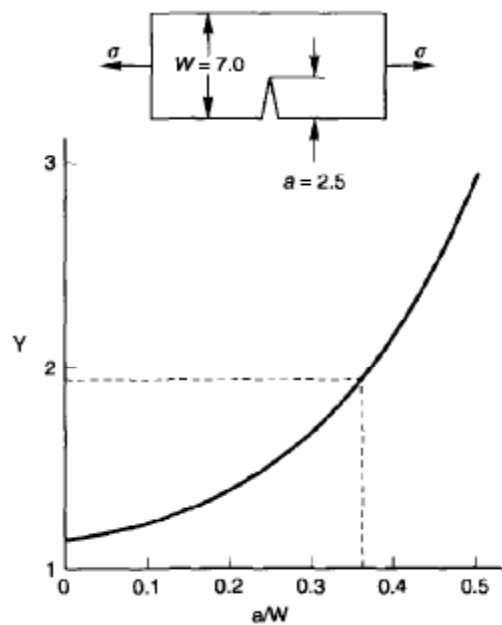


Fig. 16.3.  $Y$  value for the crack. Dimensions in mm.

The critical stress is 64% greater than the longitudinal stress. However, the change in section from a cylinder to a sphere produces something akin to a stress concentration; when this is taken into account the failure is accurately predicted.

#### Conclusions and recommendations

This case study provides a good example of the consequences of having an inadequate fracture toughness. However, even if the heat-affected zone had a high toughness, the crack would have continued to grow through the wall of the tank by stress-corrosion cracking until fast fracture occurred. The critical crack size would have been greater, but failure would have occurred eventually. The only way of avoiding failures of this type is to prevent stress corrosion cracking in the first place.

### CASE STUDY 2: COMPRESSED AIR TANKS FOR A SUPERSONIC WIND TUNNEL

The supersonic wind tunnels in the Aerodynamic Laboratory at Cambridge University are powered by a bank of twenty large cylindrical pressure vessels. Each time the tunnels are used, the vessels are slowly charged by compressors, and then quickly discharged through a tunnel. How should we go about designing and checking pressure vessels of this type to make sure they are safe?

#### Criteria for design of safe pressure vessels

First, the pressure vessel must be safe from plastic collapse: that is, the stresses must everywhere be below general yield. Second, it must not fail by fast fracture: if the largest cracks it could contain have length  $2a$  (Fig. 16.4), then the stress intensity  $K \approx \sigma\sqrt{\pi a}$  must everywhere be less than  $K_c$ . Finally, it must not fail by fatigue: the slow growth of a crack to the critical size at which it runs.

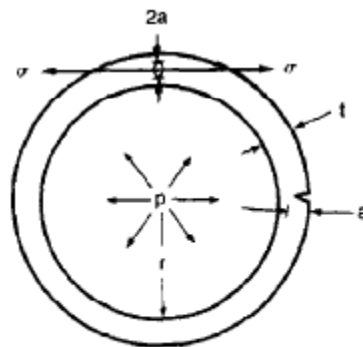


Fig. 16.4. Cracks in the wall of a pressure vessel.

The hoop stress  $\sigma$  in the wall of a cylindrical pressure vessel containing gas at pressure  $p$  is given by

$$\sigma = \frac{pr}{t},$$

provided that the wall is thin ( $t \ll r$ ).

For general yielding,

$$\sigma = \sigma_y.$$

For fast fracture,

$$\sigma\sqrt{\pi a} = K_c.$$

#### Failure by general yield or fast fracture

Figure 16.5 shows the loci of general yielding and fast fracture plotted against crack size. The yield locus is obviously independent of crack size, and is simply given by  $\sigma = \sigma_y$ . The locus of fast fracture can be written as

$$\sigma = \frac{K_c}{\sqrt{\pi}} \left( \frac{1}{\sqrt{a}} \right),$$

which gives a curved relationship between  $\sigma$  and  $a$ . If we pressurise our vessel at point A on the graph, the material will yield *before* fast fracture; this yielding can be detected by strain gauges and disaster avoided. If we pressurise at point B, fast fracture will occur at a stress less than  $\sigma_y$  without warning and with catastrophic consequences; the point where the two curves cross defines a critical flaw size at which fracture by general yield and by fast fracture coincide. Obviously, if we know that the size of the largest flaw in our vessel is less than this critical value, our vessel will be safe (although we

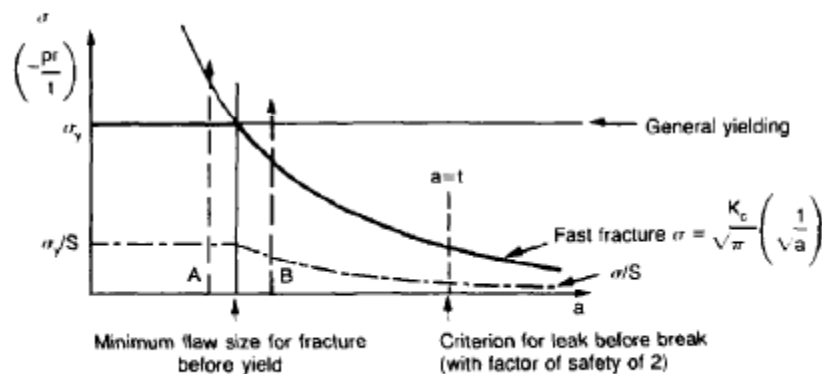


Fig. 16.5. Fracture modes for a cylindrical pressure vessel.

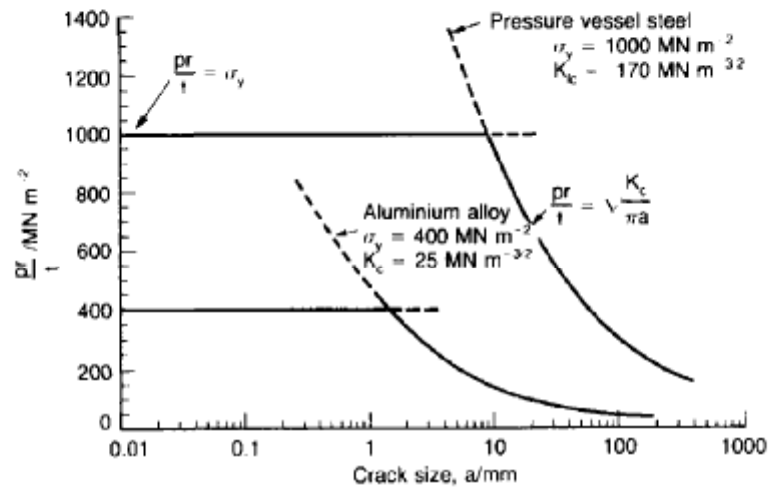


Fig. 16.6. Design against yield and fast fracture for a cylindrical pressure vessel.

should also, of course, build in an appropriate safety factor  $S$  as well – as shown by the dash – dot line on Fig. 16.5).

Figure 16.6 shows the general yield and fast fracture loci for a pressure-vessel steel and an aluminium alloy. The critical flaw size in the steel is  $\approx 9$  mm; that in the aluminium alloy is  $\approx 1$  mm. It is easy to detect flaws of size 9 mm by ultrasonic testing, and pressure-vessel steels can thus be accurately tested non-destructively for safety – vessels with cracks larger than 9 mm would not be passed for service. Flaws of 1 mm size cannot be measured so easily or accurately, and thus aluminium is less safe to use.

### Failure by fatigue

In the case of a pressure vessel subjected to *cyclic loading* (as here) cracks can grow by fatigue and a vessel initially passed as safe may subsequently become unsafe due to this crack growth. The probable extent of crack growth can be determined by making fatigue tests on pre-cracked pieces of steel of the same type as that used in the pressure vessel, and the safe vessel lifetime can be estimated by the method illustrated in Case Study 3.

### Extra safety: leak before break

It is worrying that a vessel which is safe when it enters service may become unsafe by slow crack growth – either by fatigue or by stress corrosion. If the consequences of catastrophic failure are very serious, then additional safety can be gained by designing the vessel so that it will *leak before it breaks* (like the partly inflated balloon of Chapter 13). Leaks are easy to detect, and a leaking vessel can be taken out of service and repaired. How do we formulate this leak-before-break condition?

If the critical flaw size for fast fracture is less than the wall thickness ( $t$ ) of the vessel, then fast fracture can occur with no warning. But suppose the critical size ( $2a_{crit}$ ) is

greater than  $t$  – then gas will leak out through the crack before the crack is big enough to run. To be on the safe side we shall take

$$2a_{\text{crit}} = 2t.$$

The stress is defined by

$$\sigma\sqrt{\pi a_{\text{crit}}} = K_c$$

so that the permissible stress is

$$\sigma = \frac{K_c}{\sqrt{\pi t}}$$

as illustrated on Fig. 16.5.

There is, of course, a penalty to be paid for this extra safety: either the pressure must be lowered, or the section of the pressure vessel increased – often substantially.

### Pressure testing

In many applications a pressure vessel may be tested for safety simply by hydraulic testing to a pressure that is higher – typically 1.5 to 2 times higher – than the normal operating pressure. Steam boilers (Fig. 16.7) are tested in this way, usually once a year. If failure does not occur at twice the working pressure, then the normal operating stress is at most one-half that required to produce fast fracture. If failure *does* occur under

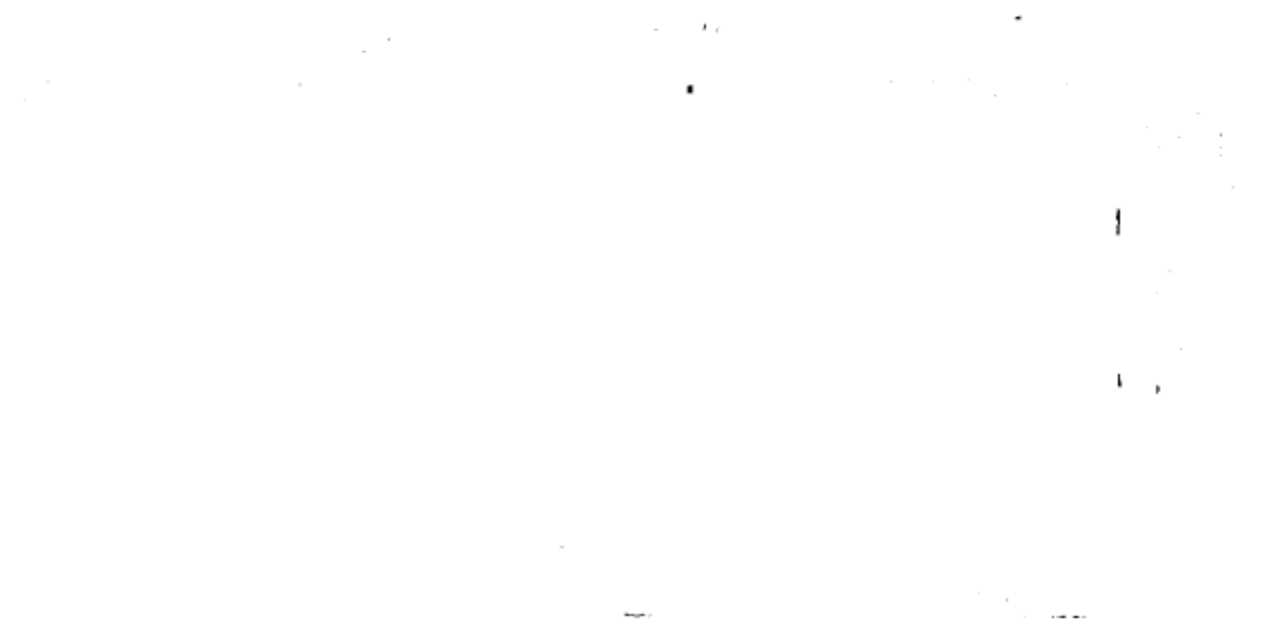


**Fig. 16.7.** A pressure vessel in action – the boiler of the articulated steam locomotive *Merddin Emrys*, built in 1879 and still hauling passengers on the Festiniog narrow-gauge railway in North Wales.

hydraulic test nobody will get hurt because the stored energy in compressed water is small. Periodic testing is vital because cracks in a steam boiler will grow by fatigue, corrosion, stress corrosion and so on.

### CASE STUDY 3: THE SAFETY OF THE STRETHAM ENGINE

The Stretham steam pumping engine (Fig. 16.8) was built in 1831 as part of an extensive project to drain the Fens for agricultural use. In its day it was one of the largest beam engines in the Fens, having a maximum power of 105 horsepower at 15 rpm (it could

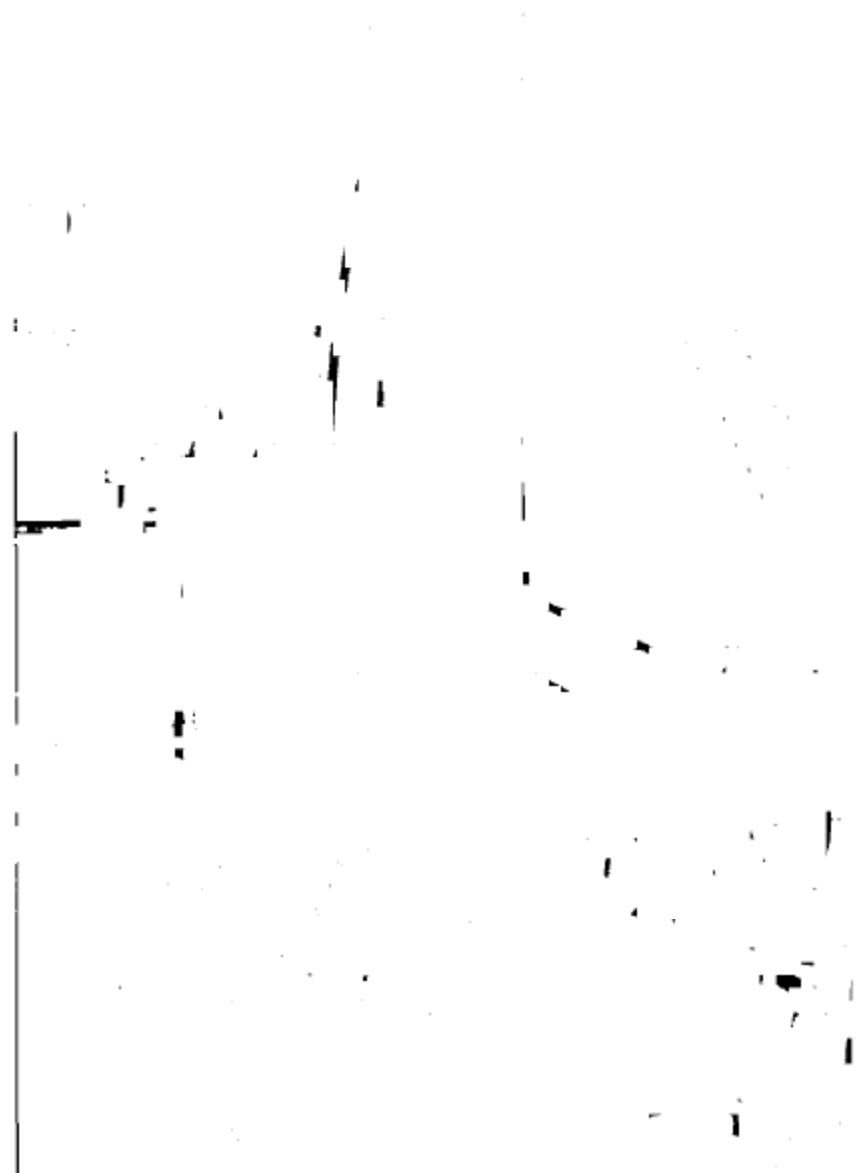


**Fig. 16.8.** Part of the Stretham steam pumping engine. In the foreground are the crank and the lower end of the connecting rod. Also visible are the flywheel (with separate spokes and rim segments, all pegged together), the eccentric drive to the valve-gear and, in the background, an early treadle-driven lathe for on-the-spot repairs.

lift 30 tons of water per revolution, or 450 tons per minute); it is now the sole surviving steam pump of its type in East Anglia.\*

The engine could still be run for demonstration purposes. Suppose that you are called in to assess its safety. We will suppose that a crack 2 cm deep has been found in the connecting rod – a cast-iron rod, 21 feet long, with a section of  $0.04 \text{ m}^2$ . Will the crack grow under the cyclic loads to which the connecting rod is subjected? And what is the likely life of the structure?

### Mechanics

The stress in the crank shaft is calculated approximately from the power and speed as follows. Bear in mind that approximate calculations of this sort may be in error by up to a factor of 2 – but this makes no difference to the conclusions reached below. Referring to Fig. 16.9:

$$\begin{aligned} \text{Power} &= 105 \text{ horsepower} \\ &= 7.8 \times 10^4 \text{ J s}^{-1}, \\ \text{Speed} &= 15 \text{ rpm} = 0.25 \text{ rev s}^{-1}, \\ \text{Stroke} &= 8 \text{ feet} = 2.44 \text{ m}, \end{aligned}$$

Force  $\times 2 \times \text{stroke} \times \text{speed} \approx \text{power}$ ,

$$\therefore \text{Force} = \frac{7.8 \times 10^4}{2 \times 2.44 \times 0.25} = 6.4 \times 10^4 \text{ N}.$$

Nominal stress in the connecting rod  $= F/A = 6.4 \times 10^4 / 0.04 = 1.6 \text{ MN m}^{-2}$  approximately.

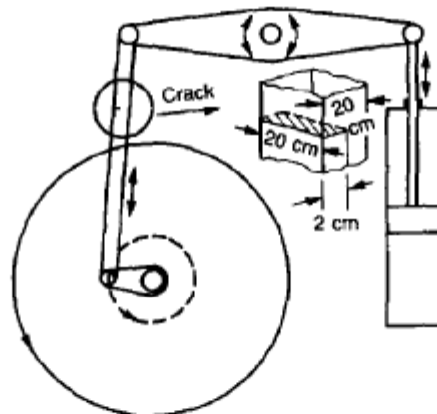


Fig. 16.9. Schematic of the Stretham engine.

\*Until a couple of centuries ago much of the eastern part of England which is now called East Anglia was a vast area of desolate marshes, or fens, which stretched from the North Sea as far inland as Cambridge.

**Failure by fast fracture**

For cast iron,  $K_c = 18 \text{ MN m}^{-3/2}$ .

First, could the rod fail by fast fracture? The stress intensity is:

$$K = \sigma\sqrt{\pi a} = 1.6\sqrt{\pi \cdot 0.02} \text{ MN m}^{-3/2} = 0.40 \text{ MN m}^{-3/2}.$$

It is so much less than  $K_c$  that there is no risk of fast fracture, even at peak load.

**Failure by fatigue**

The growth of a fatigue crack is described by

$$\frac{da}{dN} = A(\Delta K)^m. \quad (16.1)$$

For cast iron,

$$A = 4.3 \times 10^{-8} \text{ m (MN m}^{-3/2})^{-4},$$

$$m = 4.$$

We have that

$$\Delta K = \Delta\sigma\sqrt{\pi a}$$

where  $\Delta\sigma$  is the range of the tensile stress (Fig. 16.10). Although  $\Delta\sigma$  is constant (at constant power and speed),  $\Delta K$  increases as the crack grows. Substituting in eqn. (16.1) gives

$$\frac{da}{dN} = A\Delta\sigma^4\pi^2 a^2$$

and

$$dN = \frac{1}{(A\Delta\sigma^4\pi^2)} \frac{da}{a^2}.$$

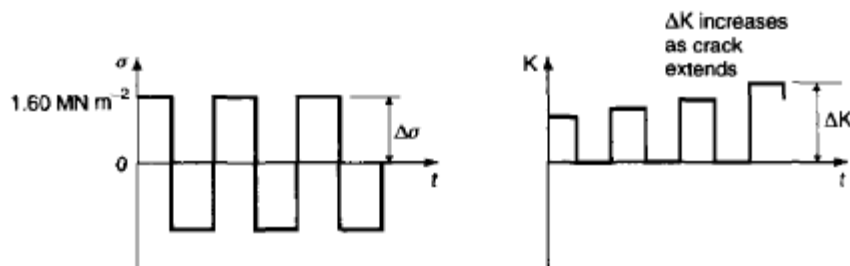


Fig. 16.10. Crack growth by fatigue in the Stretham engine.

Integration gives the number of cycles to grow the crack from  $a_1$  to  $a_2$ :

$$N = \frac{1}{(A\Delta\sigma^4 \pi^2)} \left\{ \frac{1}{a_1} - \frac{1}{a_2} \right\}$$

for a range of  $a$  small enough that the crack geometry does not change appreciably. Let us work out how long it would take our crack to grow from 2 cm to 3 cm. Then

$$\begin{aligned} N &= \frac{1}{4.3 \times 10^{-8} (1.6)^4 \pi^2} \left\{ \frac{1}{0.02} - \frac{1}{0.03} \right\} \\ &= 5.9 \times 10^6 \text{ cycles.} \end{aligned}$$

This is sufficient for the engine to run for 8 hours on each of 832 open days for demonstration purposes, i.e. to give 8 hours of demonstration each weekend for 16 years. A crack of 3 cm length is still far too small to go critical, and thus the engine will be perfectly safe after the  $5.9 \times 10^6$  cycles. Under demonstration the power delivered will be far less than the full 105 horsepower, and because of the  $\Delta\sigma^4$  dependence of  $N$ , the number of cycles required to make the crack grow to 3 cm might be as much as 30 times the one we have calculated.

The estimation of the total lifetime of the structure is more complex – substantial crack growth will make the crack geometry change significantly; this will have to be allowed for in the calculations by incorporating a correction factor,  $Y$ .

### Conclusion and recommendation

A simple analysis shows that the engine is likely to be safe for limited demonstration use for a considerable period. After this period, continued use can only be sanctioned by regular inspection of the growing crack, or by using a more sophisticated analysis.

### Further reading

- J. F. Knott, *Fundamentals of Fracture Mechanics*, Butterworths, 1973.
- T. V. Duggan and J. Byrne, *Fatigue as a Design Criterion*, Macmillan, 1977.
- R. W. Hertzberg, *Deformation and Fracture Mechanics of Engineering Materials*, 4th edition, Wiley, 1996.
- S. P. Timoshenko and J. N. Goodier, *Theory of Elasticity*, 3rd edition, McGraw Hill, 1970.

